

AD-A019 523

**RADAR SCATTERING FROM A RANDOM OCEAN SURFACE PERTURBED
BY A SURFACE CURRENT**

John Jarem, et al

Physical Dynamics, Incorporated

Prepared for:

Rome Air Development Center
Defense Advanced Research Projects Agency

August 1975

DISTRIBUTED BY:

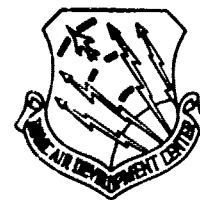
NTIS

**National Technical Information Service
U. S. DEPARTMENT OF COMMERCE**

ADA019523

C23108

RADC-TR-75-207
Interim Report
August 1975



**RADAR SCATTERING FROM A RANDOM OCEAN SURFACE
PERTURBED BY A SURFACE CURRENT**

Physical Dynamics, Inc.

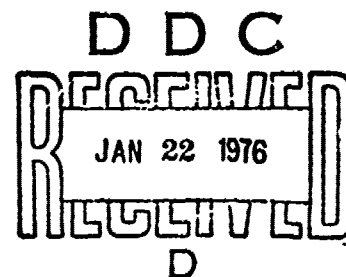
**Sponsored by
Defense Advanced Research Projects Agency
ARPA Order No. 1649**

**Approved for public release;
distribution unlimited.**

The views and conclusions contained in this document are those of the authors and should not be interpreted as necessarily representing the official policies, either expressed or implied, of the Defense Advanced Research Projects Agency or the U. S. Government.

**Rome Air Development Center
Air Force Systems Command
Griffiss Air Force Base, New York 13441**

Reproduced by
**NATIONAL TECHNICAL
INFORMATION SERVICE**
US Department of Commerce
Springfield, VA. 22151



ACCESSION for	
NTIS	White Section <input type="checkbox"/>
ODC	Self Section <input checked="" type="checkbox"/>
UNANNOUNCED	<input type="checkbox"/>
JUSTIFICATION	
BY	
DISTRIBUTION/AVAILABILITY CODES	
Dist.	AVAIL and/or SPECI:
A	

**RADAR SCATTERING FROM A RANDOM OCEAN SURFACE
PERTURBED BY A SURFACE CURRENT**

Johr. Jarem
Bruce J. West

Contractor: Physical Dynamics, Inc.
Contract Number: F30602-72-C-0494
Effective Date of Contract: 1 May 1972
Contract Expiration Date: 31 December 1975
Amount of Contract: \$598,861.00
Program Code Number: 5E20
Period of work covered: May 72 - Dec 75

Principal Investigator: J. Alex Thomson
Phone: 415 848-3063

Project Engineer: Leonard Strauss
Phone: 315 330-3055

Approved for public release;
distribution unlimited.

This research was supported by the Defense
Advanced Research Projects Agency of the
Department of Defense and was monitored by
Leonard Strauss, RADC (OCSE), Griffiss AFB
NY 13441.

DDC
RECEIVED
JAN 22 1976
REGULATED
D

UNCLASSIFIED

SECURITY CLASSIFICATION OF THIS PAGE (When Data Entered)

REPORT DOCUMENTATION PAGE		READ INSTRUCTIONS BEFORE COMPLETING FORM
1. REPORT NUMBER RADC-TR-75-207	2. GOVT ACCESSION NO.	3. RECIPIENT'S CATALOG NUMBER
4. TITLE (and Subtitle) RADAR SCATTERING FROM A RANDOM OCEAN SURFACE PERTURBED BY A SURFACE CURRENT		5. TYPE OF REPORT & PERIOD COVERED Interim Report
		6. PERFORMING ORG. REPORT NUMBER PD-74-057
7. AUTHOR(s) John Jarem Bruce J. West		8. CONTRACT OR GRANT NUMBER(s) F30602-72-C-0494
		10. PROGRAM ELEMENT, PROJECT, TASK AREA & WORK UNIT NUMBERS 62301E 16490402
9. PERFORMING ORGANIZATION NAME AND ADDRESS Physical Dynamics, Inc. P. O. Box 1069 Berkeley CA 94701		12. REPORT DATE August 1975
11. CONTROLLING OFFICE NAME AND ADDRESS Defense Advanced Research Projects Agency 1400 Wilson Blvd Arlington VA 22209		13. NUMBER OF PAGES 73
		15. SECURITY CLASS. (of this report) UNCLASSIFIED
14. MONITORING AGENCY NAME & ADDRESS (if different from Controlling Office) Rome Air Development Center (OCSE) Griffiss AFB NY 13441		15a. DECLASSIFICATION/DOWNGRADING SCHEDULE N/A
16. DISTRIBUTION STATEMENT (of this Report) Approved for public release; distribution unlimited.		
17. DISTRIBUTION STATEMENT (of the abstract entered in Block 20, if different from Report) Same		
18. SUPPLEMENTARY NOTES RADC Project Engineer: Leonard Strauss/OCSE		
19. KEY WORDS (Continue on reverse side if necessary and identify by block number) Radar Scattering Random Ocean Surface Composite Model Current Induced Perturbation		
20. ABSTRACT (Continue on reverse side if necessary and identify by block number) The scattering of radar energy from a rough ocean surface is considered using the approximations of physical optics and perturbation theory. The ocean surface is taken to be generated by a random process with zero mean value and a homogeneous covariance function represented by a wavenumber energy spectrum. For slightly rough seas the coherent and incoherent backscatter cross-sections are obtained for a general ocean spectrum. For very rough seas the physical optics cross-sections were calculated for a Gaussian ocean spectrum neglecting		

DD FORM 1 JAN 73 1473 EDITION OF 1 NOV 68 IS OBSOLETE

UNCLASSIFIED

SECURITY CLASSIFICATION OF THIS PAGE (When Data Entered)

UNCLASSIFIED

SECURITY CLASSIFICATION OF THIS PAGE(When Data Entered)

shadowing. Scattering from ripples where the ocean surface radius of curvature is no longer large compared to radar wavelength was treated by perturbation theory using the magnetic dyadic Green's function for a half plane. The scattered field perturbed by the rough surface was obtained from a perturbation expansion of the surface fluctuation. Incoherent cross-sections were found to be different for horizontal and vertical polarizations. The "visibility" of current induced perturbations for particular radar frequencies is calculated for a Phillip's saturated spectrum of surface waves.

UNCLASSIFIED

iii

SECURITY CLASSIFICATION OF THIS PAGE(When Data Entered)

TABLE OF CONTENTS

	<u>Page</u>
Title Page	i
DD 1473	ii
Table of Contents	iv
List of Figures	v
Abstract	vi
I. INTRODUCTION	1
II. PHYSICAL OPTICS SCATTERING	6
III. PHYSICAL OPTICS SCATTERING FOR SLIGHTLY ROUGH SEA	10
IV. COMPOSITE MODEL - SCALAR EQUATION	17
V. OCEAN RADAR BACKSCATTER CALCULATIONS	24
VI. CURRENT INDUCED PERTURBATION	35
VII. DISCUSSION AND CONCLUSIONS	45
References	48
Appendices	
A - Effects of Diffraction	49
B - Averages of Statistically Separable Surfaces	51
C - Physical Optics Scattering for a Rough Sea	53
D - Perturbation Theory for Scattering from a Slightly Rough Sea	55
E - Quasi-Specular Scattering from Very Rough Sea	64

LIST OF FIGURES

	<u>Page</u>	
FIGURE 1	Geometry for Rough Ocean Scattering	7
FIGURE 2	Radar Pulse Illumination of Ocean Surface	16
FIGURE 3	Scattering Geometry with Incident Wave in the (x,z) plane.	19
FIGURE 4	Schematic of Energy Contained in Surface Waves of the Oceans - $\phi(f)$ is the Energy Spectrum as a Function of Frequency	25
FIGURE 5	Final Smoothed Spectrum from Project SWOP Measurements, $\phi(k,\theta)$ is the Energy Spectrum as a Function of Wavevector (Ft^4).	28
FIGURE 6	One-Dimensional Wavenumber Spectrum taken along North-South Direction in SWOP Contours of Figure 5.	29
FIGURE 7	Radar Cross Sections are depicted as a Function of Angle of Incidence θ_0 for a Phillip's Saturated Spectrum Using: i.) the Quasi-Spectular Scattering Model $\sigma_{Q.S.}$, (ii) the Physical Optics Scattering Model $\sigma_{P.O.}$ and iii) Perturbation Theory with Vertical ($\sigma_{V.V.}$) and Horizontal ($\sigma_{H.H.}$) Polarizations.	33
FIGURE 8	Incoherent Scattering Function $\Psi(a,\beta)$ for an Ocean Surface with a Gaussian Correlation Function.	54
FIGURE 9	Scattering Geometry with Incident Wave in the (x,z) Plane and a Smooth Ocean Surface (S_0) and Displaced Surface (S).	56

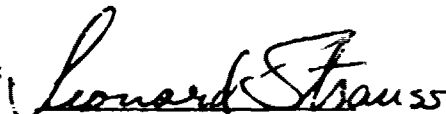
ABSTRACT

The scattering of radar energy from a rough ocean surface is considered using the approximations of physical optics and perturbation theory. The ocean surface is taken to be generated by a random process with zero mean value and a homogeneous covariance function represented by a wavenumber energy spectrum. For slightly rough seas the coherent and incoherent backscatter cross-sections are obtained for a general ocean spectrum. For very rough seas, the physical optics cross-sections were calculated for a Gaussian ocean spectrum neglecting shadowing. Scattering from ripples where the ocean surface radius of curvature is no longer large compared to radar wavelength was treated by perturbation theory using the magnetic dyadic Green's function for a half plane. The scattered field perturbed by the rough surface was obtained from a perturbation expansion of the surface fluctuation. Incoherent cross-sections were found to be different for horizontal and vertical polarizations. The "visibility" of current induced perturbations for particular radar frequencies is calculated for a Phillip's saturated spectrum of surface waves.

This report has been reviewed by the RADC Information Office (OI) and is releasable to the National Technical Information Service (NTIS). At NTIS it will be releasable to the general public including foreign nations.

This report has been reviewed and is approved for publication.

APPROVED:



LEONARD STRAUSS
Project Engineer

Do not return this copy. Retain or destroy.

I. INTRODUCTION

The standard treatments of radar scattering from the ocean surface generally assume i) that this surface wave field has an incoherent hydrodynamic interaction and is therefore describable by a spectrum, and ii) that this spectrum may be partitioned into a part with waves of low curvature and a part with waves of low amplitudes. Callen and Dashen¹ argue this separation at a wavenumber k_c by comparing the mean square radius of curvature for the long waves R^2 and the mean square height of the short waves h^2 to the radar wavelength λ_r . The conditions $h/\lambda_r \ll 1$ and $\lambda_r/R \ll 1$ are then satisfied simultaneously. The short waves are the scattering centers and ride on the longer waves. The scattering of scalar electromagnetic waves from the short water waves is treated in linear perturbation theory and the undulating surface on which the scatterers ride by geometric optics.

Calculations by Lane² indicate that the dominant effect of the longer waves is to provide a tilted surface on which the scattering centers ride. Wright³ calculates the effect of the long waves ($k < k_c$) by averaging over the tilt angle of the surface in determining the scattered radiation. The general expression for the radar cross section of the surface can be written as

$$\sigma(\theta) = \iint P(\phi, \psi) S(\theta, \phi, \psi) G(\phi, \psi) \phi(\vec{k}, \theta) d\phi d\psi \quad (1)$$

where $P(\phi, \psi) d\phi d\psi$ is the probability that the surface is tilted at angles between ϕ and $\phi+d\phi$ in the x and between ψ and $\psi+d\psi$ in the y directions, respectively. This function $P(\phi, \psi)$ could equivalently have been written in terms of the surface slopes in the x and y direction. Wright uses the distribution in tilt angles determined by the glint measurements of Cox and Munk⁴. The covariance of this distribution is taken to be a linear function of wind speed measured 12.5 m above the ocean surface. The radar cross section then becomes a function of sea state as well as the angle of incidence of the radar (θ).

A second effect of the long waves and one included in the second term under the integral is the phenomenon of shadowing. Shadowing is a function of surface slope rather than curvature and therefore has contributions from both the long and short waves. This phenomenon is the blocking of electromagnetic waves by one segment of ocean surface so that they do not reach a second segment of ocean. If this effect is dependent only on the angle of incidence and the local slope of the surface, then it may be described by a function $S(\theta, \phi, \psi)$. The arguments used in constructing the shadowing function (S) are stochastic so that one seeks the probability that a given segment of

the ocean will be in the shadow of another for a given angle of incidence.

In Beckmann⁵ this probability is related to the shadow function $S(\theta)$ for scattering from a random rough surface. This function is zero on the shadowed parts of the surface and unity on the illuminated sections. A section of the surface with unit area will present a reduced area $S(\theta)$ (<1) available for scattering when shadowing is present.

Bass, et al.⁶, discuss the radar cross section as a function of angle of incidence implementing various assumptions about the statistics of the longer waves, i.e., $k < k_c$. A shadowing function is obtained by averaging over the fluctuations of the longer waves and the sensitivity to the statistical character of the longer waves is studied. The radar cross section (σ) is expressed in terms of a scattering integral which includes the shadowing function in the integrand. This result is formally exact, subject to the general restrictions noted in the Callen-Dahsen analysis.

The third term under the integral in Eq. (1) is a geometric factor determined by the boundary conditions for electromagnetic scattering from an inclined surface. This factor is clearly a function of the incident ray angle and the tilt of the surface, i.e., the slope.

The last factor in Eq. (1) is the spectral density function for the small wave structure at the ocean surface ($k > k_c$). It is, of course, this structure which gives rise to the backscattered radiation and provides the "random rough surface" assumed to be present in the discussions of the shadowing function. These explicit assumptions about the independent and stationary character of the statistics of the short and long waves are questionable. The modulation of the short wavelength spectrum by waves near the spectral peak is discussed in Watson and West⁷, but no systematic analysis of the effect on the statistics of the short waves yet exists.

The treatments of shadowing mentioned above have all neglected diffraction^{2,3,5,6}. The effect of diffraction, using the mean square slope of the ocean surface as a parameter, is discussed in Appendix A.

In this report we shall be concerned in part with the vector scattering of radar waves from a random ocean using the approximations of physical optics and perturbation theory. The surface $\zeta(\vec{x}, t)$ is taken to be a random function continuous in the mean with a specified correlation function of surface heights. The correlation function is characterized by the sea surface spectrum for the short wavelength waves. The scattered far field is related to the incident radar wave by an approximate form of the Stratton-Chu theory.

In the physical optics approximation, the basic assumption is that every point of the rough ocean surface reflects the incident wave like an infinite tangent plane. At radar frequencies, the surface is perfectly conducting. Shadowing and multiple scattering effects are neglected.

II. PHYSICAL OPTICS SCATTERING

The electromagnetic field scattered from an area of ocean S is given by⁸

$$\vec{E}(\vec{r}) = \int_S dS \left\{ \hat{n} \times \left(\nabla' \times [\vec{E}_0(\vec{r}') + \vec{E}(\vec{r}')] \right) \right\} \cdot \vec{G}(\vec{r}-\vec{r}') \quad (2.1)$$

where $\vec{E}(\vec{r})$ is the scattered field at receiver point \vec{r} , S the illuminated ocean surface, \hat{n} the local surface normal, and $\vec{E}_0(\vec{r}')$ the incident radar field at a point \vec{r}' on the surface. The free-space dyadic Green's function is

$$\begin{aligned} \vec{G}(\vec{r}-\vec{r}') &= \left(\vec{\delta} + \frac{\nabla \nabla}{k^2} \right) \exp(-k|\vec{r}-\vec{r}'|) / 4\pi |\vec{r}-\vec{r}'| \\ &\xrightarrow{r \rightarrow \infty} \left(\vec{\delta} - \hat{r} \hat{r} \right) \exp[-ik(r-\hat{r} \cdot \vec{r}')] / 4\pi r \end{aligned} \quad (2.2)$$

The scattering geometry is shown in Figure 1.

If the far field approximation is used in Eq. (2.1) we obtain

$$\begin{aligned} E_i(\vec{r}) &= \frac{i}{2\pi r} \exp(-ikr) k E_0 P_{ij} \int_S dS \hat{n}_j \exp[-i(\vec{k}-k\hat{r}) \cdot \vec{r}'] \\ P_{ij} &= (\delta_{ij} - \hat{r}_i \hat{r}_j) \left[\hat{k}_i \hat{E}_j^{(0)} - \hat{k}_j \hat{E}_i^{(0)} \right] \end{aligned} \quad (2.3)$$

where the tensor P_{ij} contains all polarization information.

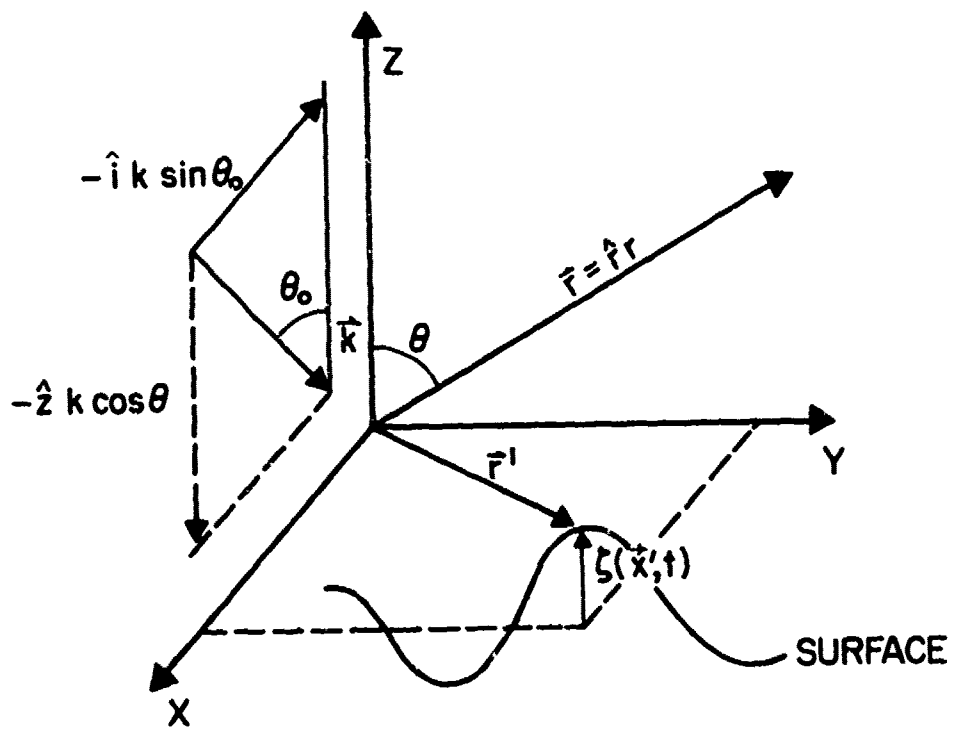


FIG. 1

GEOMETRY FOR ROUGH OCEAN SCATTERING

We note that due to the partitioning of effects, ensemble averaging can be applied directly to the surface integral in Eq. (2.3) free of polarization.

To express the surface integral [call it $\hat{I}(\hat{r})$] in terms of the surface height random variable $\zeta(\vec{x}')$, the surface displacement is assumed to be a first order quantity, i.e., the long waves are essentially flat so that

$$\begin{aligned}\vec{r}' &= \hat{x}x' + \hat{y}y' + \hat{z}\zeta(\vec{x}') \\ \hat{n} &= \frac{\nabla' [z' - \zeta(\vec{x}')] }{|\nabla(z' - \zeta)|}\end{aligned}\quad (2.4)$$

and an element of area on the inclined surface is

$$dS = |\nabla(z' - \zeta)| dx' dy' \quad (2.5)$$

When Eqs. (2.4) and (2.5) are used in the stochastic integral,

$$\hat{I}(\hat{r}) = \int_S dx' dy' \left(\hat{z} - \hat{x} \frac{\partial \zeta}{\partial x'} - \hat{y} \frac{\partial \zeta}{\partial y'} \right) \exp \left\{ -i (\vec{k} - k\hat{r}) \cdot [\hat{x}x' + \hat{y}y' + \hat{z}\zeta(\vec{x}')] \right\} \quad (2.6)$$

For the important case of backscatter, $\vec{k} - k\hat{r} = 2\vec{k}$, and denoting the incident polarization by $\hat{E}_0 = \hat{q}$, we obtain

$$\vec{E}(\vec{r}) = \frac{ikE_0}{2\pi r} \hat{k} \cdot \hat{I}(\vec{r}) \exp(-ikr)$$

$$= \frac{-ikE_0 \exp(-ikr)}{2\pi r} \hat{q} \int_S dx' dy' \left[\cos\theta_0 - \sin\theta_0 \frac{\partial \zeta(\vec{x}')}{\partial x'} \right]$$

$$\times \exp[i2k(x' \sin\theta_0 + \zeta \cos\theta_0)] \quad . \quad (2.7)$$

III. PHYSICAL OPTICS SCATTERING FOR SLIGHTLY ROUGH SEA

The integral in Eq. (2.7), call it I , is the basis for our study of radar scattering from a rough ocean. If we square and average the scattered field, we obtain the mean backscattered power as a function of incidence angle θ_0 . We note that correlations of heights and slopes of the sea surface must be known to evaluate the backscattered power. In this section we assume the roughness height to be small ($k\sigma_z \ll 1$) and any correlation distance to be much greater than the wavelengths of the scattering centers.

The mean radar cross section is defined by

$$\sigma \equiv 4\pi r^2 \left\langle \left| \frac{\vec{E}(\vec{r})}{\vec{E}_i(\vec{r})} \right|^2 \right\rangle = \frac{k^2}{\pi} \langle |I|^2 \rangle \quad (3.1)$$

and can be expressed as the sum of the coherent (σ_c) and incoherent (σ_I) cross sections

$$\begin{aligned} \sigma_c &\equiv 4\pi r^2 \left| \frac{\langle \vec{E}(\vec{r}) \rangle}{\vec{E}_i(\vec{r})} \right|^2 = \frac{k^2}{\pi} |\langle I \rangle|^2 \\ \sigma_I &\equiv \frac{k^2}{\pi} \left(\langle |I|^2 \rangle - |\langle I \rangle|^2 \right) \end{aligned} \quad (3.2)$$

Averaging over the square of the integral part of Eq. (2.7) yields

$$\langle |I|^2 \rangle = \int_S \exp[i2k \sin\theta_0(x_1-x_2)] dx_1 dx_2 dy_1 dy_2$$

$$\left\{ \mathcal{C}_1 \cos^2\theta_0 + [\mathcal{C}_2^{(1)} - \mathcal{C}_2^{(2)}] \cos\theta_0 \sin\theta_0 + \mathcal{C}_3 \sin^2\theta_0 \right\}. \quad (3.3)$$

If the statistical fluctuations in the surface displacement $[\zeta(\vec{x})]$ are homogeneous and Gaussian with zero mean, then in terms of the correlation function $\sigma_z^2 E(x_1-x_2, y_1-y_2)$, we have

$$\mathcal{C}_1 \equiv \langle \exp[i2k \cos\theta_0(\zeta_1 - \zeta_2)] \rangle = \exp[-(2k\sigma_z \cos\theta_0)^2 (1-E)]$$

$$\mathcal{C}_2^{(1)} \equiv \left\langle \frac{\partial \zeta_1}{\partial x_1} \exp[i2k \cos\theta_0(\zeta_1 - \zeta_2)] \right\rangle = -i2k\sigma_z^2 \frac{\partial E}{\partial x_1}$$

$$\times \exp[-(2k\sigma_z \cos\theta_0)^2 (1-E)]$$

$$\mathcal{C}_3 \equiv \left\langle \frac{\partial \zeta}{\partial x_1} \frac{\partial \zeta}{\partial x_2} \exp[i2k \cos\theta_0(\zeta_1 - \zeta_2)] \right\rangle = \left[\sigma_z^2 \frac{\partial^2 E}{\partial x_1 \partial x_2} \right.$$

$$\left. + (2k \cos\theta_0 \sigma_z)^2 \sigma_z^2 \frac{\partial E}{\partial x_1} \frac{\partial E}{\partial x_2} \right] \exp[-(2k\sigma_z \cos\theta_0)^2 (1-E)] \quad (3.4)$$

where $\mathcal{C}_2^{(2)}$ is obtained by interchanging 1 and 2 in the expression for $\mathcal{C}_2^{(1)}$ and $\zeta_\ell \equiv \zeta(x_\ell, y_\ell)$; $\ell = 1, 2$.

Using these results in Eq. (3.3) we obtain after some reduction

$$\langle |I|^2 \rangle = \exp\left[-(2k\sigma_z \cos\theta_0)^2\right] \int_S dx_1 dx_2 dy_1 dy_2 \exp\left[i2k \sin\theta_0 (x_1 - x_2)\right] \\ \left\{ \left[\cos^2\theta_0 - \frac{\tan^2\theta_0}{4k^2} \frac{\partial^2}{\partial x_1^2} + \frac{i \sin\theta_0}{k} \frac{\partial}{\partial x_1} \right] \exp\left[(2k\sigma_z \cos\theta_0)^2 E\right] \right\}. \quad (3.5)$$

A similar computation shows

$$\langle I \rangle = \cos\theta_0 \exp\left[-\frac{1}{2}(2\sigma_z \cos\theta_0)^2\right] \int_S dx_1 dy_1 \exp(i2 \sin\theta_0 x_1) \quad (3.6)$$

where we have used

$$\langle \exp(i2k\zeta \cos\theta_0) \rangle = \exp\left[-\frac{1}{2}(2k\sigma_z \cos\theta_0)^2\right]$$

$$\left\langle \frac{\partial \zeta}{\partial x_1} \exp(i2k\zeta \cos\theta_0) \right\rangle = 0 \quad .$$

For small root mean square (rms) fluctuations in surface height,

$$\alpha \equiv (2k\sigma_z \cos\theta_0)^2 \ll 1 \quad ,$$

Eq. (3.5) can be approximated by

$$\langle |I|^2 \rangle \cong \exp(-\alpha) \int_S dx_1 \dots dy_2 \left[\cos^2\theta_0 (1 + \alpha E) - (\sigma_z \sin\theta_0)^2 \frac{\partial^2 E}{\partial x_1^2} \right. \\ \left. + i4k\sigma_z^2 \sin\theta_0 \cos^2\theta_0 \frac{\partial E}{\partial x_1} \right] \exp\left[i2k \sin\theta_0 (x_1 - x_2)\right] . \quad (3.7)$$

The two-point correlation function E can be expressed as the Fourier Transform of the energy density of ocean surface waves $\phi(\vec{k})$,

$$E(x_1-x_2, y_1-y_2) = \int_{-\infty}^{\infty} d\vec{k} \phi(\vec{k}) \exp\left\{i\left[\kappa_1(x_1-x_2) + \kappa_2(y_1-y_2)\right]\right\}. \quad (3.8)$$

Using this representation and assuming the illuminated surface area to be large in both dimensions, we obtain after integration over S

$$\begin{aligned} \langle |I|^2 \rangle \exp(\alpha) &= \cos^2 \theta_0 C^2(\hat{x}2k \sin \theta_0) \\ &+ \alpha \cos^2 \theta_0 \int_{-\infty}^{\infty} d\vec{k} \phi(\vec{k}) C^2(\vec{k} + \hat{x}2k \sin \theta_0) \\ &+ (\sigma_z \sin \theta_0)^2 \int_{-\infty}^{\infty} d\vec{k} \kappa_1^2 \phi(\vec{k}) C^2(\vec{k} + \hat{x}2k \sin \theta_0) \\ &- 4k \sigma_z^2 \sin \theta_0 \cos^2 \theta_0 \int_{-\infty}^{\infty} d\vec{k} \kappa_1 \phi(\vec{k}) C^2(\vec{k} + \hat{x}2k \sin \theta_0) \quad (3.9) \end{aligned}$$

where

$$C(\vec{k}) \equiv \int_S dx dy \exp\left[i(\kappa_1 x + \kappa_2 y)\right].$$

We note that $C(\vec{k})$ is sharply peaked about $\vec{k} = 0$ for a large surface and approaches a delta function as $S \rightarrow \infty$. Making use of this property, we obtain the following approximation for Eq. (3.9):

$$\langle |I|^2 \rangle \exp(\alpha) = \cos^2 \theta_0 C^2(\hat{x}2k \sin \theta_0) + (2\pi)^2 S(2k\sigma_z)^2 \phi(-x2k \sin \theta_0). \quad (3.10)$$

On squaring Eq. (3.6) we obtain

$$|I|^2 = \cos^2 \theta_0 \exp(-\alpha) C^2(\hat{x}2k \sin \theta_0) \quad (3.11)$$

so that using Eqs: (3.10) and (3.11) in Eq. (3.2), the incoherent cross section per unit area is

$$\frac{\sigma_I}{S} = 16\pi (k^2 \sigma_z)^2 \exp[-(2k\sigma_z \cos \theta_0)^2] \phi(-\hat{x}2k \sin \theta_0) \quad (3.12)$$

The coherent cross section per unit area is, similarly,

$$\frac{\sigma_C}{S} = \frac{k^2}{\pi} \cos^2 \theta_0 \exp[-(2k\sigma_z \cos \theta_0)^2] \frac{C^2(\hat{x}2k \sin \theta_0)}{S} \quad (3.13)$$

The rough ocean surface is much larger than the area illuminated by the radar antenna beam. The field strength over the illuminated area is not uniform but varies according to the gain pattern. We shall assume that the field is uniform over the half power angular beam width θ_B and zero

outside. For moderately large angles of incidence, the geometry is shown in Figure 2. The radar pulse is τ seconds in duration, c is the velocity of light, and r is slant range to the illuminated area. The rough surface area contributing to the backscattered power is one-half of the illuminated area or

$$S = \frac{1}{2} A_I = \frac{1}{2} c \theta_B r \tau \quad (3.14)$$

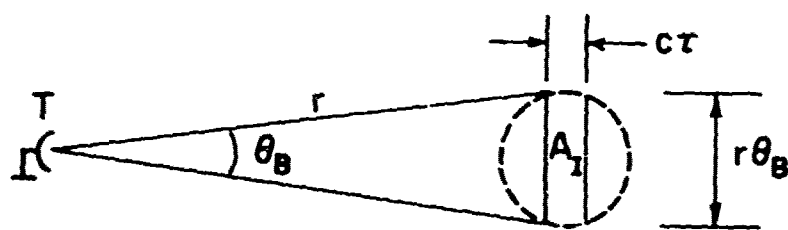
If the illuminated area is approximately rectangular with dimensions $x_0 = r \theta_B$ and $y_0 = \frac{c\tau}{2}$, then

$$C(\hat{x}2k \sin\theta_0) = S \operatorname{sinc}(kx_0 \sin\theta_0) \quad (3.15)$$

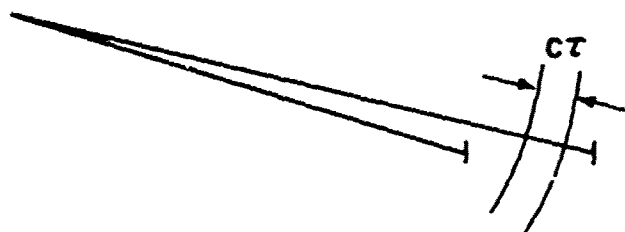
and the coherent cross section per unit area is

$$\frac{\sigma_c}{S} = \frac{k^2 S}{\pi} \cos^2 \theta_0 \exp\left[-(2k\sigma_z \cos\theta_0)^2\right] \operatorname{sinc}^2(kx_0 \sin\theta_0) \quad (3.16)$$

Since $\lambda_r/x_0 \ll 1$, the coherent cross section is unimportant off normal incidence.



TOP VIEW



SIDE VIEW

FIG. 2

RADAR PULSE ILLUMINATION OF OCEAN SURFACE

IV. COMPOSITE MODEL - SCALAR EQUATION

In Section II, it was shown that the effect of polarization factors from the integral determining the scattered electric field [see Eq. (2.7)]. A direct evaluation of the scattering integral, which is a scalar, in terms of an ensemble average was than made in Section III to determine the dependence of the scattered field on the spectrum of scatterers and the undulating surface. In this section, we extend the investigation of Callen and Dashen¹ on the scattering of a scalar wave from a rough surface to obtain an explicit dependence of the clutter cross section on the spectrum of long waves. The analysis follows that of reference (1) until the evaluation of the scattering integral is made. At this point, Callen and Dashen use the stationary phase approximation to evaluate the integral, whereas we make explicit assumptions about the statistics of the long wave amplitudes and about the energy spectrum to simplify the integral.

In the investigation of Callen and Dashen the vector field given by Eq. (2.1) is replaced by the scalar equation,

$$E^{(1)}(\vec{X}) = -k^2(n-1) \int d\vec{\rho} \zeta_1(\vec{\rho}) G_0[\vec{X}, \vec{X}'(\vec{\rho})] E^{(0)}[\vec{X}(\vec{\rho})] \quad (4.1)$$

where the total field is given by the perturbation expansion

$$E(\vec{r}) = \sum_p E^{(p)}(\vec{r}) \quad (4.2)$$

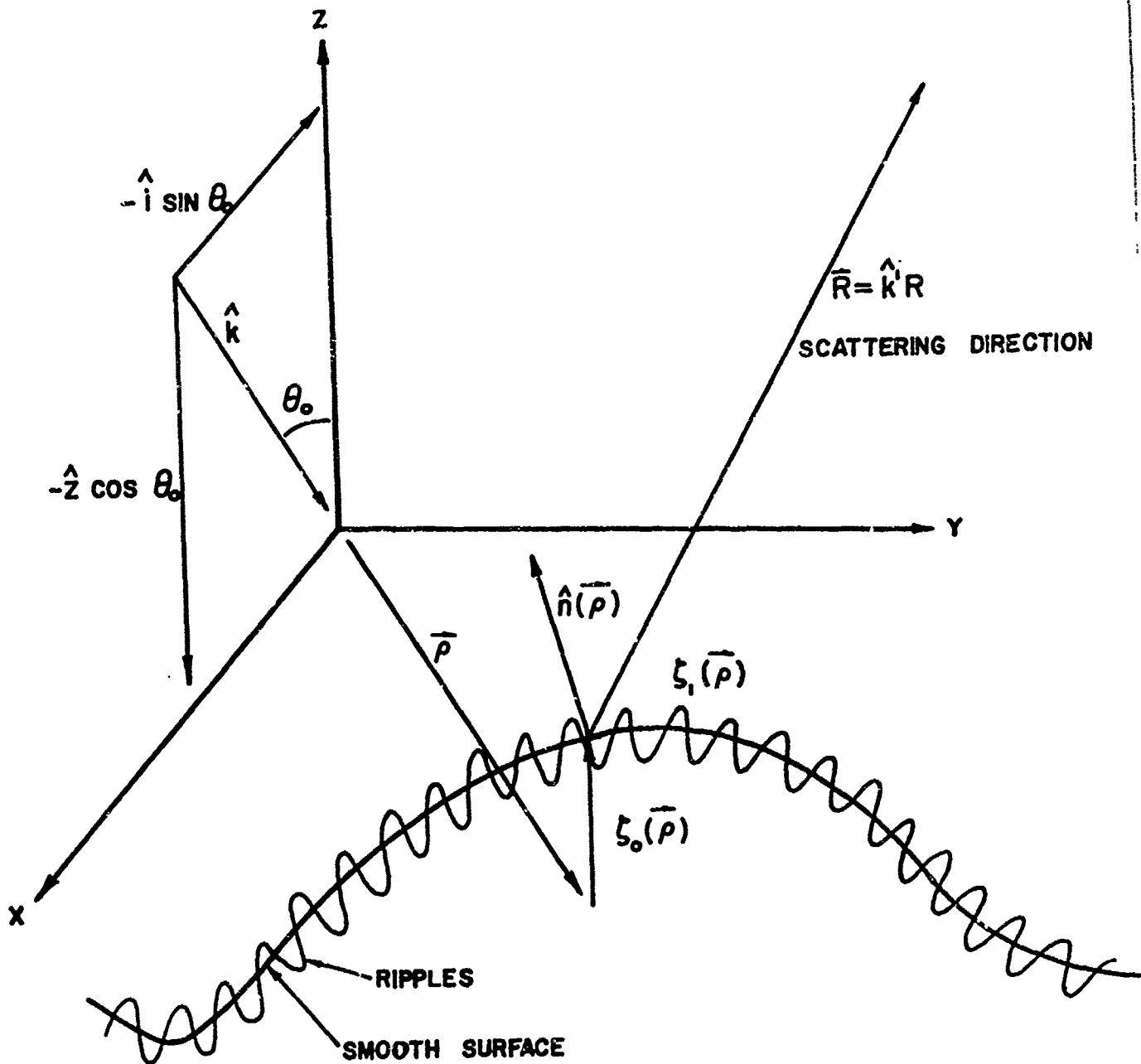
$E^{(p)} \sim |\zeta|^p$, ζ being the surface displacement and n the dielectric constant for sea water. The surface has been separated into a long and short wavelength part with displacements $\zeta_0(\vec{\rho})$ and $\zeta_1(\vec{\rho})$, respectively, as shown in Figure 3. The vector $\vec{\rho} \equiv (x, y)$ locates a point on the surface $z = 0$, and $\vec{\chi}(\vec{\rho}) \equiv (\vec{\rho}, \zeta_0(\vec{\rho}))$ locates a point on the undulating surface $z = \zeta_0(\vec{\rho})$.

Using the Greens' function from reference (1) and the unperturbed scalar field in Eq.(4.1), we obtain the far field expression,

$$E^{(1)}(\hat{k}'R) = \frac{k^2(n-1)}{4\pi R} \int d\vec{\rho} \zeta_1(\vec{\rho}) T(\alpha) T(\alpha') \exp\left[ik(\hat{k}-\hat{k}') \cdot \vec{\chi}(\vec{\rho})\right] \quad (4.3)$$

with the geometric factor

$$T(\alpha) = \frac{2 \cos\alpha}{\cos\alpha + \sqrt{n - \sin^2\alpha}} \quad (4.4)$$



SCATTERING GEOMETRY WITH INCIDENT WAVE IN THE (X,Z) PLANE

FIGURE 3

arising from the boundary condition for the electromagnetic wave at the undulating surface. For backscatter $\hat{k}' = -\hat{k}$ and $\cos\alpha' = \cos\alpha = \hat{k}' \cdot \hat{n}$, so that

$$T(\alpha)T(\alpha') \approx \frac{4 \cos^2 \alpha}{n + 2\sqrt{n}} \quad (4.5)$$

where the denominator differs from the exact expression by less than 1% for $n = 80$.

The integral in Eq. (4.3) may be changed to a surface integral over the illuminated surface $\zeta_0(\vec{\rho})$ by introducing $\bar{\zeta}_1$ which is the normal distance between the surface ζ_0 and $\zeta_0 + \zeta_1$. We then have $d\vec{\rho}\zeta_1(\vec{\rho}) \rightarrow dS \bar{\zeta}_1(x,y)$. Letting $Z(x,y) \equiv \zeta_0(x,y)$, we have for the unit normal to $Z(x,y)$,

$$\hat{n} = \frac{\nabla Z}{|\nabla Z|} = \frac{\hat{z} - \hat{x} Z_x - \hat{y} Z_y}{\sqrt{1 + Z_x^2 + Z_y^2}} \quad (4.6)$$

the unit area

$$dS = \sqrt{1 + Z_x^2 + Z_y^2} dx dy \quad (4.7)$$

the cosine of the local angle of incidence

$$\cos\alpha = \hat{k} \cdot \hat{n} = \frac{Z_x \sin\theta_0 - \cos\theta_0}{\sqrt{1 + Z_x^2 + Z_y^2}} \quad (4.8)$$

and the normal surface displacement

$$\bar{\zeta}_1(\vec{\rho}) = \zeta_1(\vec{\rho}) \sqrt{1 + z_x^2 + z_y^2} \quad (4.9)$$

Using Eq.(4.7) - (4.9) in eq (4.3) yields for the back-scattered perturbed field

$$E^{(1)}(-\hat{k}R) = \frac{k^2(n-1)}{\pi(n+2\sqrt{n})R} \int dx \int dy \zeta_1(x,y) \left[\cos^2\theta_0 + z_x^2 \sin^2\theta_0 - z_x \sin 2\theta_0 \right] \times \exp \left[-i2k(x \sin\theta_0 + z(x,y) \cos\theta_0) \right] \quad (4.10)$$

Using Eq. (4.10), we introduce the function $f_0(\vec{\rho})$ defined by

$$f_0(\vec{\rho}) \equiv (\cos^2\theta_0 + z_x^2 \sin^2\theta_0 - z_x \sin 2\theta_0) \exp \left[-i2k(x \sin\theta_0 + z \cos\theta_0) \right] \quad (4.11)$$

so that upon squaring and averaging (4.10) over an appropriate ensemble we obtain

$$\langle |E^{(1)}|^2 \rangle = \frac{k^4}{\pi^2 R^2} \left(\frac{n-1}{n+\sqrt{n}} \right)^2 \int d\vec{\rho} \int d\vec{\rho}' \langle \zeta_1(\vec{\rho}) \zeta_1(\vec{\rho}') \rangle \langle f_0(\vec{\rho}) f_0^*(\vec{\rho}') \rangle \quad (4.12)$$

In Eq.(4.12) we have assumed that the ripples (ζ_1) are statistically independent of the long waves (f_0).

In the following analysis, we assume a Gaussian ocean surface for the long waves and that

$$\langle z(\vec{\rho}) z(\vec{\rho}') \rangle = \sigma_z^2 E_z(\vec{\rho} - \vec{\rho}') \quad (4.13)$$

where

$$\sigma_z^2 \equiv \langle z^2(\vec{\rho}) \rangle \quad (4.14)$$

and E_z is the correlation function for the long waves.

Using the notation $z = z(\vec{\rho})$, $z' = z(\vec{\rho}')$ and $K = -2k \cos \theta_0$, we have

$$\begin{aligned} \langle f_0(\vec{\rho}) f_0^*(\vec{\rho}') \rangle = & \exp[-i2k(x-x') \sin \theta_0] \left\{ \cos^4 \theta_0 \langle \exp[iK(z-z')] \rangle \right. \\ & + \sin^2 \theta_0 \cos^2 \theta_0 \langle (z_x^2 + z_{x'}'^2) \exp[iK(z-z')] \rangle \\ & - \cos^2 \theta_0 \sin 2\theta_0 \langle (z_x + z_{x'}') \exp[iK(z-z')] \rangle \\ & - \sin^2 \theta_0 \sin 2\theta_0 \langle z_x z_{x'}', (z_{x'}' + z_x) \exp[iK(z-z')] \rangle \\ & + \sin^4 \theta_0 \langle z_x^2 z_{x'}'^2 \exp[iK(z-z')] \rangle \\ & \left. + \sin^2 2\theta_0 \langle z_x z_{x'}' \exp[iK(z-z')] \rangle \right\} \quad (4.15) \end{aligned}$$

The averages defined by eq (4.15) are evaluated in Appendix B for gentle long waves.

We introduce the function $F(\vec{\rho}-\vec{\rho}';\theta_0)$ by the right hand side of eq (4.15), as follows

$$\langle f_0(\vec{\rho}) f_0^*(\vec{\rho}') \rangle \equiv F(\vec{\rho}-\vec{\rho}';\theta_0) \exp[-i2k(x-x') \sin\theta_0] \quad (4.16)$$

Equation (4.16) may be used to evaluate the integral in (4.12) when the ripple correlation length is small compared to the long wave correlation length, i.e., the correlation of short waves is essentially a delta function on the scale of the long wave, so that

$$\begin{aligned} \langle |E^{(1)}|^2 \rangle &\approx \frac{.65k^4}{\pi^2 R^2} F(\vec{\ell};\theta_0) \int d\vec{\rho} \int d\vec{\rho}' \langle \zeta_1(\vec{\rho}) \zeta_1(\vec{\rho}') \rangle \\ &\times \exp[-i2k \sin\theta_0 (x-x')] \end{aligned} \quad (4.17)$$

where $|\vec{\ell}|$ is the correlation length of the short waves. The integral defines the spectrum of short waves at $\Delta\vec{k} = (2k \sin\theta_0, 0)$, $\vec{r} = \vec{\rho} - \vec{\rho}'$, yielding for the clutter cross section

$$\begin{aligned} \sigma^{(1)} &= \frac{R^2 \langle |E^{(1)}|^2 \rangle}{S} \\ &\approx 2.61k^4 F(\vec{\ell};\theta_0) \phi(-\Delta\vec{k}, \vec{r}) \end{aligned} \quad (4.18)$$

where S is the illuminated area. The cross section for scattering from the long waves as given in reference⁽¹⁾ is unchanged.

V. OCEAN RADAR BACKSCATTERING CALCULATIONS

In the preceding sections and in Appendices C, D, and E, a number of distinct models for the scattering of electromagnetic waves from ocean surfaces of varying degrees of roughness are presented. The models have been based on different combinations of the four conditions: (i) that the roughness height be smaller than the radar wavelength illuminating the surface ($k\sigma_z \ll 1$), (ii) any correlation distance for the short waves is smaller than their wavelengths ($k\ell \ll 1$), (iii) the local mean square slope be small ($\sigma_{\text{sea}}^2 \ll 1$) and (iv) the root mean square radius of curvature of the long waves is much greater than the radar wavelength ($\lambda_r/R \ll 1$). Condition (iv) is a restriction in all the models discussed.

The applicability of the above models to various wave-number regimes and sea states will be explored in this section. Also, the statistical parameters which characterize the ocean surface will be discussed for a variety of representations of the ocean wave spectrum.

In Figure 4, we show a schematic of an ocean energy spectrum. We note especially that the frequency region of interest for radar returns spans both gravity and capillary waves. The Pierson-Moskowitz spectrum⁹ gives a good representation of observed properties of wind generated gravity waves in deep water,

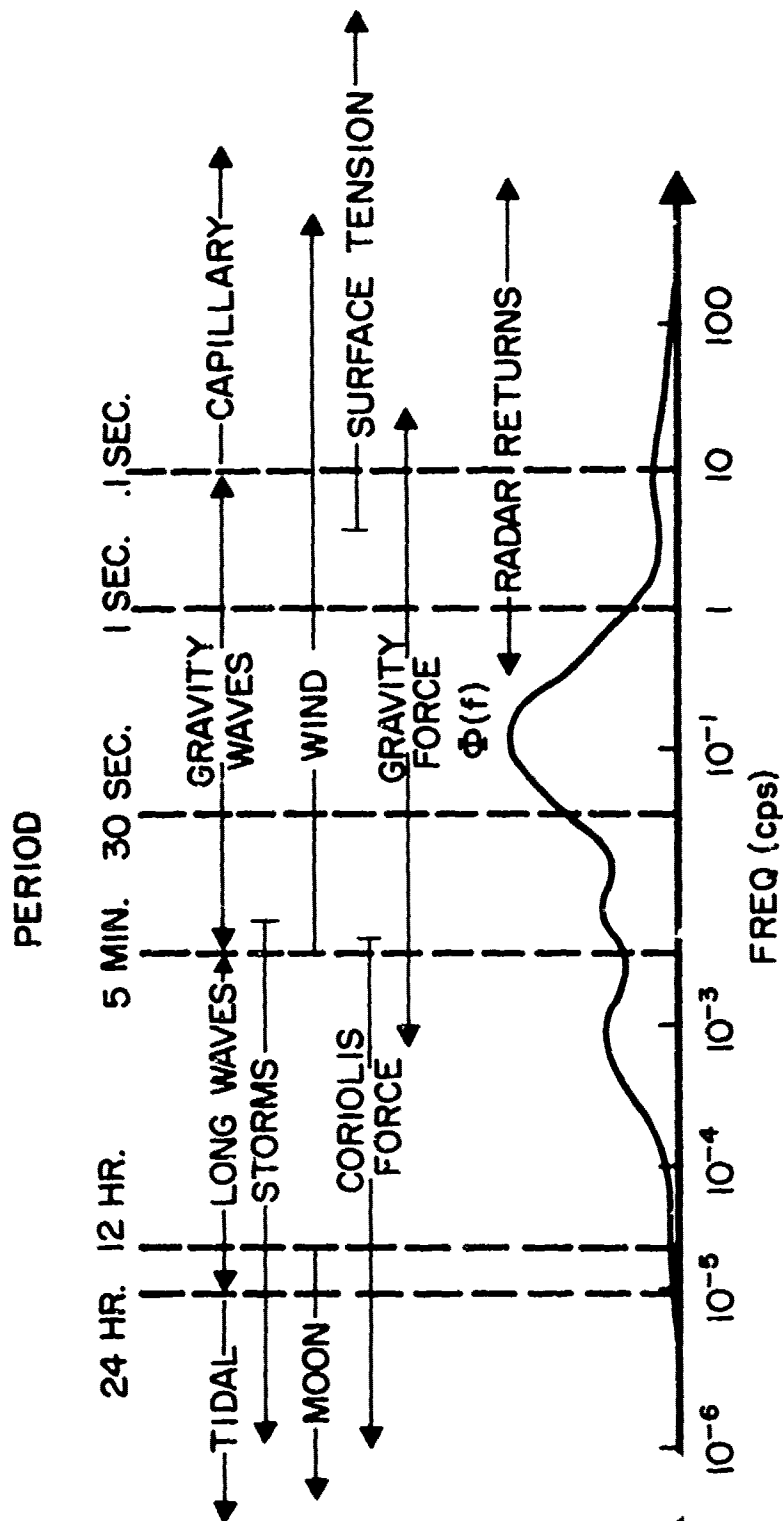


FIG. 4 SCHEMATIC OF ENERGY CONTAINED IN SURFACE WAVES OF THE OCEANS --
 $\Phi(f)$ ENERGY SPECTRUM

$$\phi(\omega) = \frac{\alpha g}{\omega^5} \exp\left[-\beta(g/U\omega)^4\right] \quad (5.1)$$

where in cgs units, $g = 980 \text{ cm/sec}^2$, U is the wind speed (cm/sec) and α and β are dimensionless constants with the values 8.1×10^{-3} and $.74$, respectively. Descriptions such as Eq. (5.1) are not as useful as they could be, however, since most theoretical discussion of the evolution of the surface wave field is in terms of the wavenumber spectrum^{10,11,12}. Using the relation

$$\phi(\omega) d\omega = \pi k dk \phi^{(2)}(k) \quad (5.2)$$

where $\phi^{(2)}(k)$ is the two-dimensional wavenumber spectrum and the linear dispersion relation for gravity waves $\omega = \sqrt{gk}$, we obtain

$$\phi^{(2)}(k) = \frac{\alpha}{2\pi k} \exp(-\beta g^2/U^4 k^2) \quad (5.3)$$

which, neglecting the exponential, yields the Phillips saturated spectrum¹³.

In Project SWOP¹⁴ a stereo technique from two airplanes was used to measure the two-dimensional wavenumber spectrum. The measurements were made over the Atlantic ocean (25 Oct 54, 39°N , 63.5°W) over an area $2700 \text{ ft} \times 1800 \text{ ft}$. Wind speeds ranged over 13-20 knots during the preceding 14 hours so that the spectral cut-off frequency in Eq. (5.1)

ranged over .444 to .10 cps. An average frequency of .29 cps was used to determine a cut-off wavelength $\lambda = \frac{2\pi g}{\omega^2} = 61$ ft. Figure 5 shows the final smoothed spectrum. Figure 6 shows the one-dimensional wavenumber spectrum taken along the north-south direction in Figure 5. Numerical integration of the latter curve leads to a mean square surface height fluctuation of $\sigma_z^2 = 6.75 \text{ ft}^2$ and a lower bound for the mean square slope of $\phi_{\text{sea}}^2 = 8.35 \times 10^{-3}$. For $\kappa > .02 \text{ ft}^{-1}$, the data indicated an excellent κ^{-4} fit. The analytical expression for the two-dimensional spectrum is

$$\begin{aligned} \phi^{(2)}(\kappa) &= 1.9 \times 10^5 \kappa^{-4.95}, \quad .0026 < \kappa < .02 \text{ ft}^{-1} \\ \phi^{(2)}(\kappa) &= .53 \times 10^{-3} \kappa^{-4}, \quad .02 < \kappa < 60 \text{ ft}^{-1} \end{aligned} \quad (5.4)$$

yields $\sigma_z^2 = 6.75 \text{ ft}^2$ with a peak $\phi(.02) = 3300 \text{ ft}^4$.

In the wavelength region 1 to 50 cm, recent measurements¹⁵ on the NELC Tower indicate that the ocean spectrum follows a power law $\kappa^{-\alpha}$. SRI wire gauge measurements¹⁵ indicate that the one-dimensional spectrum can be approximated by the power law

$$\phi^{(1)}(\kappa) \equiv \kappa \phi^{(2)}(\kappa) = 5 \times 10^{-3} \kappa^{-3}, \quad .125 < \kappa < 2\pi \text{ cm}^{-1} \quad (5.5)$$

where $\phi^{(1)}(\kappa)$ is the one-dimensional spectrum ($\text{cm}^3/\text{radian}$).

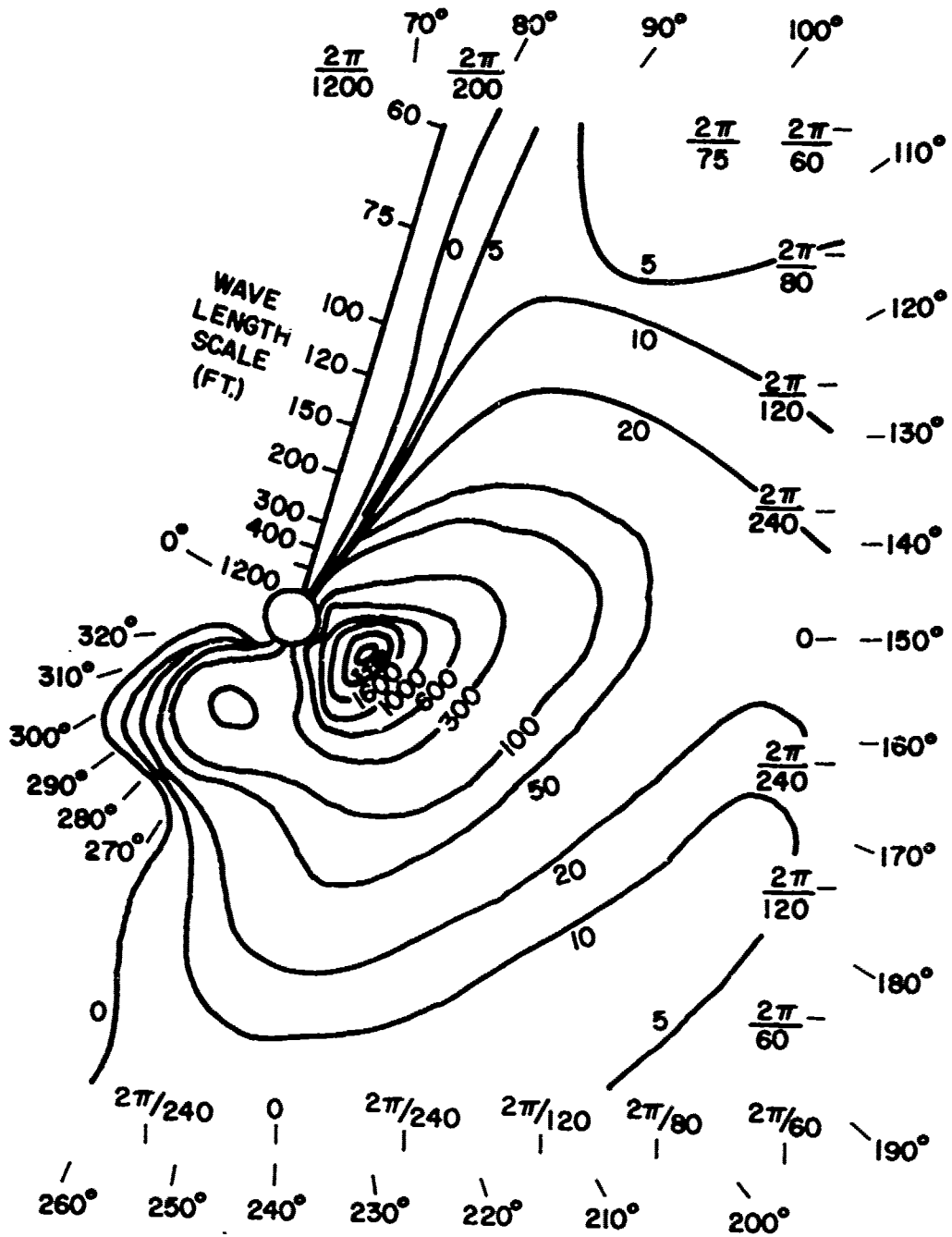
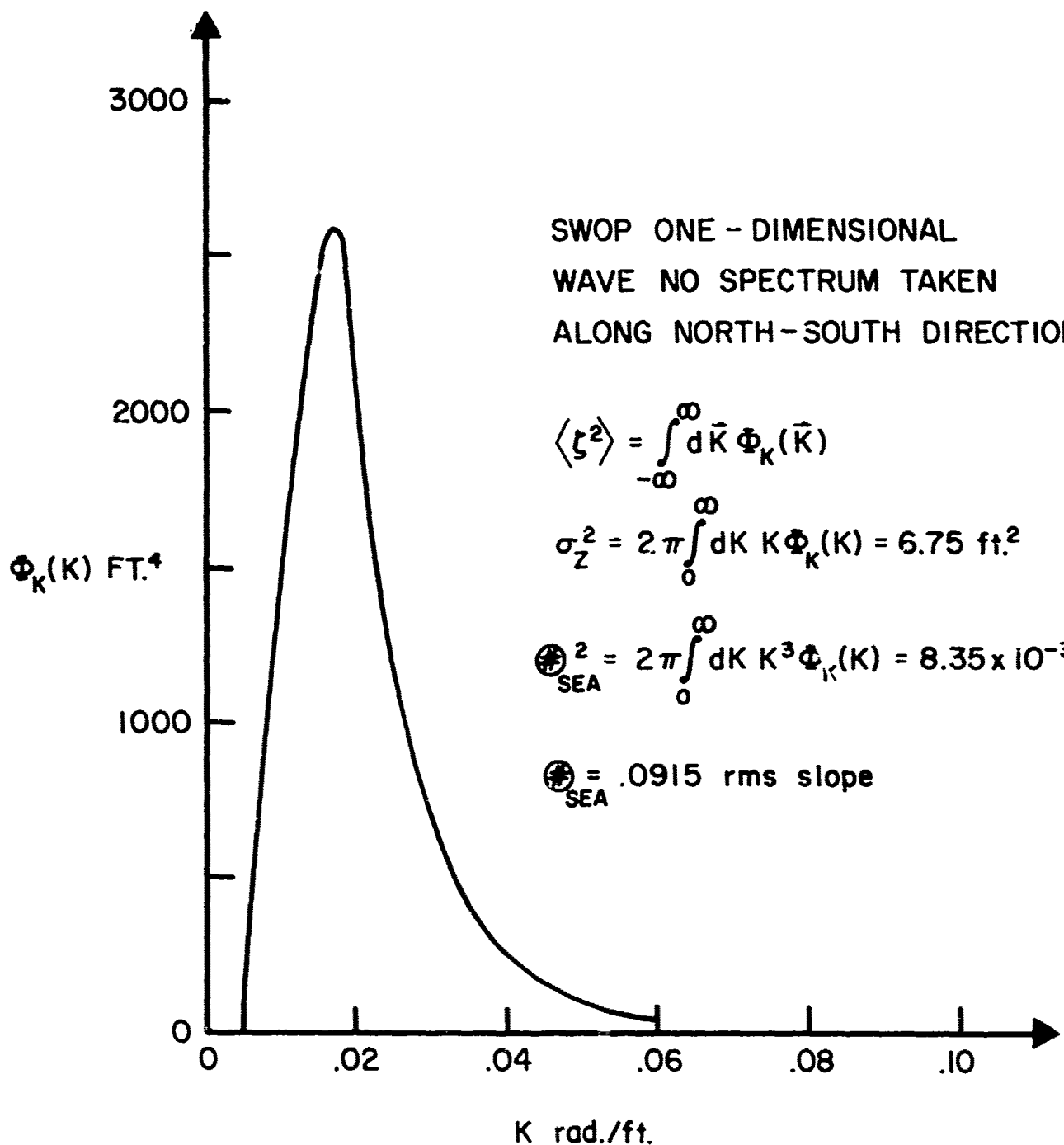


FIG. 5. FINAL SMOOTHED SPECTRUM FROM SWOP
 $\Phi(k, \theta)$ FT.⁴



ONE-DIMENSIONAL WAVENUMBER SPECTRUM TAKEN ALONG NORTH-SOUTH
DIRECTION IN SWOP CONTOURS OF FIGURE 5
FIG. 6

RRI measurements¹⁵ using a TV technique indicate an ocean spectrum approximated by

$$\begin{aligned} \phi^{(1)}(\kappa) &= 7.82 \times 10^{-5} \kappa^{-4}, \quad .125 < \kappa < 2\pi \text{ cm}^{-1} \\ &= 0, \quad \text{otherwise} \end{aligned} \quad (5.6)$$

It is interesting to compare the rms sea height (σ_z) and rms sea slope ($\textcircled{1}_{\text{sea}}$) for this small sea roughness regime to the corresponding SWOP rough sea parameters.

For the RRI spectrum

$$\begin{aligned} \sigma_z^2 &= 2\pi \int_{.125}^{2\pi} d\kappa (7.82 \times 10^{-5} \kappa^{-4}) = 8.28 \times 10^{-2} \text{ cm}^2 \\ \sigma_z &= .289 \text{ cm} \end{aligned}$$

and

$$\textcircled{1}_{\text{sea}} = .0621. \quad (5.7)$$

A correlation length (l) appropriate to this measurement is estimated assuming a Gaussian distribution of amplitudes, so that

$$\textcircled{1}_{\text{sea}}^2 = 4\sigma_z^2 / l^2 \quad (5.8)$$

yielding a correlation distance of 9.21 cm. For the SRI spectrum $\sigma_z = 1$ cm, $\textcircled{1}_{\text{sea}} = .351$ and $l = 5.71$ cm.

In Table I are collected the statistical parameters for the four ocean spectra discussed and for three radar wavelengths of interest, UHF, C band and X band. This table can be used to determine which of the radar scattering models discussed is appropriate for, (i) the radar wavelength being used, 60 cm, 6 cm or 1.6 cm, and (ii) the sea state as described by the four different spectra. It is clear, for example, that only the scattering model in Appendix E with $k\sigma_z \gg 1$ and $kl \gg 1$ is appropriate for the conditions of SWOP for any of the radar wavelengths.

In Figure 7 the cross section per unit area is plotted vs. angle of incidence for three distinct sea states. In the SWOP measurement, as pointed out above, $k\sigma_z \gg 1$ and $kl \gg 1$, so that the sea state is heavy and the scattering is quasi-spectacular. From Appendix E, the cross section for arbitrary radar wavelength is

$$\sigma_{QS}^o \equiv \frac{\sigma_I}{S} = \frac{\sec^4 \theta_o}{2 \sigma_{sea}} \exp \left[- \tan^2 \theta_o / \sigma_{sea}^2 \right] . \quad (5.9)$$

The second sea state considered is that of an equilibrium or Phillips spectrum. Perturbation theory for horizontal and vertical polarization from Appendix D yields

TABLE I

		SWOP	SRI	PHILLIPS	RRI
$\lambda=60$ cm $k=.1047$ cm ⁻¹	σ_z (cm)	65.7	1.002	.448	.289
	$k\sigma_z$	6.88	.1049	.0469	.0303
	\oplus_{sea}	.0915	.351	.157	.0621
	l (cm)	1440	5.71	5.71	9.31
	kl	150.8	.598	.548	.975
$\lambda=6$ cm $k=1.047$ cm ⁻¹	σ_z (cm)	65.7	1.002	.448	.289
	$k\sigma_z$	68.8	1.049	.469	.303
	\oplus_{sea}	.0915	.351	.157	.0621
	l (cm)	1440	5.71	5.71	9.31
	kl	1508	5.98	5.98	9.75
$\lambda=1.5$ cm $k=4.19$ cm ⁻¹	σ_z (cm)	65.7	1.002	.448	.289
	$k\sigma_z$	275.3	4.20	1.88	1.211
	\oplus_{sea}	.0915	.351	.157	.0621
	l (cm)	1440	5.71	5.71	9.31
	kl	6033	23.9	23.9	39.0

The statistical parameters, $\sigma_z \equiv$ rms height of the surface, $l \equiv$ correlation distance, $\oplus_{\text{sea}} \equiv$ rms surface slope, and $k =$ radar wavenumber ($\equiv 2\pi/\lambda$) for the four ocean spectra, SWOP, SRI, Phillips and RRI for three radar wavelengths of interest UHF (60 cm), C band (6 cm), and X band (1.5 cm) are listed.

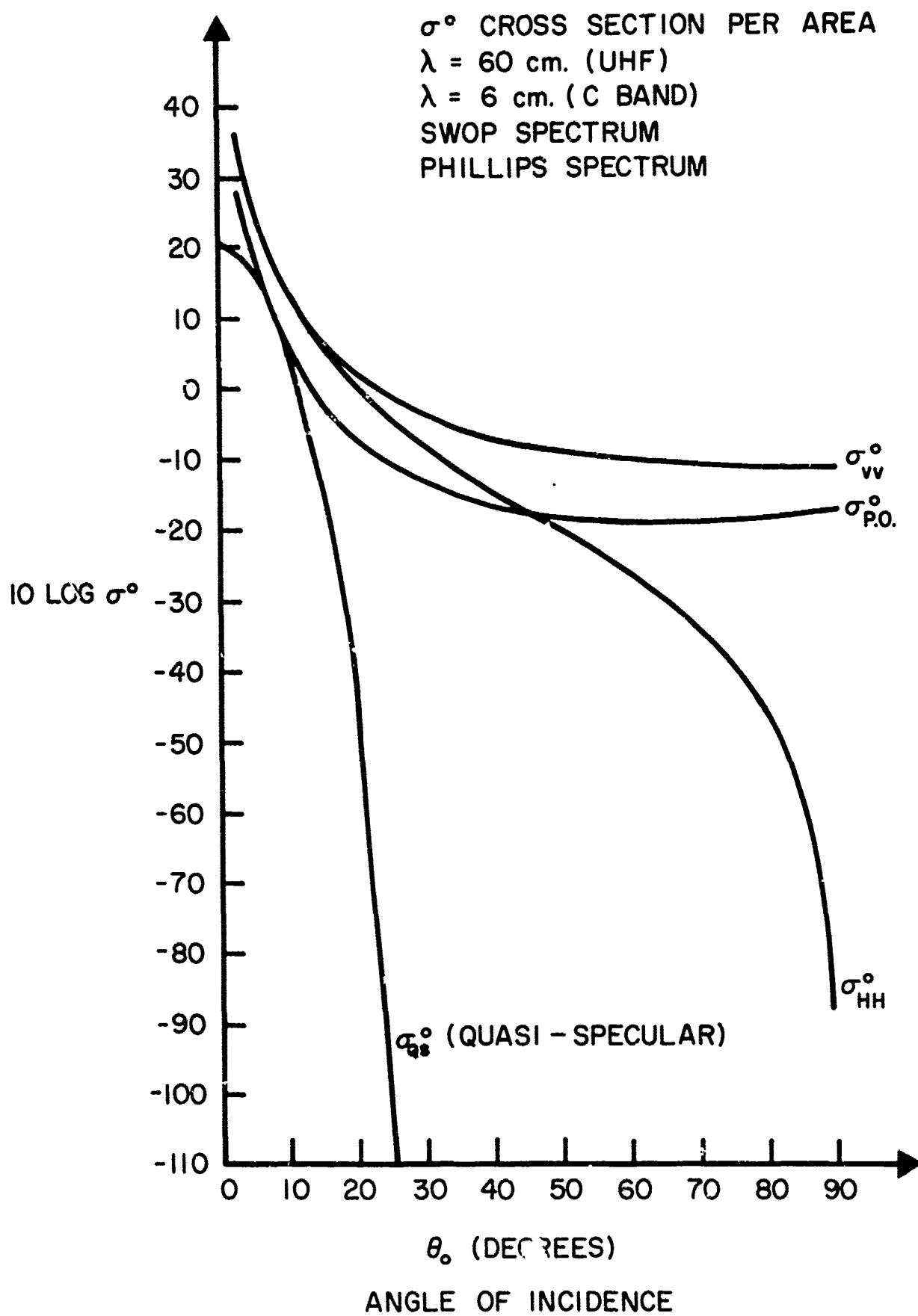


FIG. 7

$$\sigma_{HH}^o \equiv \left(\frac{\sigma_I}{S} \right)_{HH} = 16\pi k^4 \cos^4 \theta_o \phi(2k \sin \theta_o, 0)$$

$$\sigma_{VV}^o \equiv \left(\frac{\sigma_I}{S} \right)_{VV} = 16\pi k^4 [1 + \sin^2 \theta_o]^2 \phi(2k \sin \theta_o, 0) .$$

(5.10)

The distinction between vertical and horizontal polarization shows up clearly for large angles of incidence in Figure 7.

The final example is the physical optics approximation made in Section III for a slightly rough sea. Using a Phillips spectrum yields the cross section

$$\sigma_{P.O.}^o \equiv \frac{\sigma_I}{S} = 16\pi k^4 \exp [-(2k\sigma_z \cos \theta_o)^2] \phi(2k \sin \theta_o, 0)$$

(5.11)

which in Figure 7 is seen to correspond closely to the cross section for horizontally-polarized radar in Eq. (5.10).

VI. CURRENT-INDUCED PERTURBATION

The composite model discussed in Section IV enables one to separate the variable surface effects from the direct scattering effects in first order. For example, consider the surface current generated by an internal wave propagating at 50 cm/sec. A 64 cm surface wave has a group velocity equal to the internal wave phase velocity. A linear analysis, e.g., Thomson and West⁶ or Case, Watson and West⁷ would predict a resonant transfer of energy from the internal wave to the surface wave spectrum. The waves in this resonant region would therefore be strongly perturbed. The visibility of this perturbation to short wavelength radar, e.g., X-band corresponding to 3.6 cm surface waves, would be given by the perturbation in the long wave spectral function $F(\vec{\ell}; \theta_0)$ in Eq. (4.18).

In addition to the direct variation of $F(\vec{\ell}; \theta_0)$ (when the long waves are perturbed by a current) is a cascade of the perturbation to shorter wavelengths. In this process, the current modulates the longer waves which in turn modulate the shorter waves, thereby inducing a variation in $\Phi(-\Delta\vec{k}, \vec{r})$ in Eq. (4.18).

To examine the effect on the clutter cross section of the current-induced spectral perturbation, we follow Watson and West¹⁸ and introduce the power spectrum of the surface

displacement $\zeta(\vec{x}, t)$ at a position \vec{x}

$$F(\vec{x}, \vec{k}) = \frac{1}{2} \sum_{\vec{\Delta}} \langle a^*(\vec{k} + \vec{\Delta}/2) a(\vec{k} - \vec{\Delta}/2) \rangle \exp(i\vec{\Delta} \cdot \vec{x}) \quad (6.1)$$

where $a(\vec{k})$ is the time dependent amplitude of the complex surface displacement $Z(\vec{x})$,

$$Z(\vec{x}) \equiv \sum_{\vec{k}} a(\vec{k}) \exp(i\vec{k} \cdot \vec{x}) \quad (6.2)$$

and

$$\zeta(\vec{x}, t) = \frac{i}{2} [Z(\vec{x}) - Z^*(\vec{x})] . \quad (6.3)$$

To use the continuum wavenumber variables, we define the spectral function, over a surface area S ,

$$\Phi(\vec{x}, \vec{k}) = \frac{S}{(2\pi)^2} F(\vec{x}, \vec{k}) \quad (6.4)$$

with the normalization

$$\int d^2k \Phi(\vec{x}, \vec{k}) = \langle \zeta^2(\vec{x}) \rangle . \quad (6.5)$$

If the mode amplitude for the complex surface displacement in the presence of a surface current $[a(\vec{k})]$ is distinguished from that in the absence of the current $[A(\vec{k})]$, then introducing an envelope function $G_{\vec{k}}^{\vec{x}}(\vec{x}, t)$, the two amplitudes are related by

$$a(\vec{k}) = G_{\vec{k}}^{\vec{x}}(\vec{x}, t) A(\vec{k}) . \quad (6.6)$$

If the surface current is assumed to be "turned on" at time $t=0$ then $G_{\vec{k}}(\vec{x}, 0) = 1$. We can employ these amplitudes to construct the "ambient" power spectrum, i.e., the power spectrum with no current present,

$$F_a(\vec{x}, \vec{k}) = \frac{1}{2} \sum_{\vec{\Delta}} \langle A(\vec{k} + \vec{\Delta}/2) A^*(\vec{k} - \vec{\Delta}/2) \rangle \exp(i\vec{\Delta} \cdot \vec{x}) \quad (6.7)$$

The perturbed spectrum is discussed in Watson and West¹⁸ and can be written in terms of the continuous spectrum $\phi(\vec{x}, \vec{k})$ in the weak current case in the following forms:

(i) The near resonance case;

$$\begin{aligned} \frac{\delta\phi(\vec{x}, \vec{k})}{\phi_a(\vec{k})} &\approx \frac{1}{2}(U_0 kt) \cos^2\theta \sin k\xi + \frac{1}{2}(U_0 kt)^2 \cos k\xi (1 - t/\tau_p)^2 / S_p \\ &+ 2 \left(\frac{t}{\tau_p} \right)^2 \sin \left[2S_p^{1/8} \sin k\xi \right] / \sin k\xi \\ &- k \frac{\partial}{\partial k_x} (\ln \phi_a) \left[t k U_0 \sin k\xi \right] \end{aligned} \quad (6.8)$$

(ii) The far from resonance case;

$$\begin{aligned} \frac{\delta\phi(\vec{x}, \vec{k})}{\phi_a(\vec{k})} &\approx \frac{U_0 \cos k\xi}{2(C_I - C_g \cos\theta)^2} \left[C_I (\cos\theta - 2) + 2 C_g \cos\theta (1 - \cos\theta) + C_g \cos^3\theta \right] \\ &- k \frac{\partial}{\partial k_x} (\ln \phi_a) \left[\frac{U_0 \cos k\xi \cos\theta}{C_I - C_g \cos\theta} \right] \end{aligned} \quad (6.9)$$

(iii) Wavelengths very short compared to those near resonance;

$$\frac{\delta\phi(\vec{x}, \vec{k})}{\phi_a(\vec{k})} \approx \frac{U_0 \cos k\xi}{2C_I} (\cos\theta - 2) + \frac{1}{2} \int d^2L \frac{\phi_a(\vec{L})}{\phi_a(\vec{k})} L^2 (\hat{k} \cdot \hat{L}) \operatorname{Re} \left[G_L^+ - 1 \right]$$

$$\frac{-k}{C_I} \frac{\partial}{\partial k_x} (\ln \phi_a) U_0 \cos k\xi \cos\theta \quad . \quad (6.10)$$

A number of assumptions enter the construction of Eqs. (6.8)

- (6.10): (i) The surface current is harmonic, ie., $U = U_0 \cos k\xi$, $\xi = x - C_I t$ and is sufficiently weak to couple only the nearest neighbor modes in wavenumber space; (ii) The ambient spectrum is independent of position, ie., $\phi_a(\vec{x}, \vec{k}) \equiv \phi_a(\vec{k})$, (iii) the resonance wavenumber k_r is specified by the condition $C_I = C_g(k_r) \cos\theta$ and (iv) the resonance region extends over a range $\Delta k = K S_p^{1/2}$ where S_p is the parameter measuring the perturbation strength¹⁷

$$S_p = 2 \left(\frac{k_r}{k} \right)^2 \frac{U_0}{C_I (3 \cos^2\theta - 2)} \quad . \quad (6.11)$$

The time parameter in Eq. (6.8) is

$$\tau_p = \frac{\pi}{2} S_p^{1/2} / U_0 k_r \quad . \quad (6.12)$$

and $\phi_a(\vec{L})$ is the ambient long wavelength spectrum.

The variation in the clutter cross section induced by the surface current can be obtained from Eq. (4.18) to first order as

$$\frac{\delta\sigma}{\sigma} = \left(\frac{\delta F}{F}\right)_{\text{resonant}} + \left(\frac{\delta\phi}{\phi}\right)_{\text{non-resonant}} \quad (6.13)$$

The first term in Eq. (6.13) is the induced perturbation in the long wave spectrum by the surface current. Using Appendix B, we may approximate this term by

$$\left(\frac{\delta F}{F}\right)_{\text{resonant}} \approx 1 - \exp\left[-(K\sigma_z)^2 (E'_z - E_z)\right] \quad (6.14)$$

so that using Eqs. (4.13) and (6.7) we obtain

$$\left(\frac{\delta F}{F}\right)_{\text{resonant}} \approx 1 - \exp\left[-K^2 \int d^2L \delta\phi(\vec{x}, \vec{L})\right] \quad (6.15)$$

Equation (6.15) may be evaluated by substituting for the resonant perturbation of the long wave spectrum, Eq. (6.8).

As an application, we choose for the ambient spectrum, Phillips equilibrium spectrum,¹³

$$\phi_a(\vec{k}) = \frac{B}{\pi} |\vec{k}|^{-4}, \quad \vec{k} \text{ within } 90^\circ \text{ of wind direction}$$

$$B = 4 \times 10^{-3} \quad (6.16)$$

Thus,

$$k \frac{\partial}{\partial k_x} \left[\ln \phi_a(\vec{k}) \right] = -4 \cos\theta \quad (6.17)$$

Following Watson and West¹⁸ we choose parameters to correspond to typical oceanographic conditions:

$$U_0 = 10^{-2} \text{ m/sec}$$

$$\kappa = 10^{-2} \text{ m}^{-1}$$

$$k_r = 8.66 \text{ m}^{-1}$$

$$C_I = .50 \text{ m/sec}$$

$$\theta = 20^\circ \tag{6.18}$$

Here k_r is resonant wavenumber defined by $C_I = C_g \cos\theta$. The strength parameter S_p is

$$S_p = 4.609 \times 10^4 \tag{6.19}$$

the resonant time is

$$\tau_r = \frac{2}{k_r U_0} = 23.09 \text{ sec} \tag{6.20}$$

and the width of the resonance region is,

$$\Delta k = \kappa S_p^{1/2} = 2.147 \text{ m}^{-1} \tag{6.21}$$

For the Phillips' spectrum the term involving an integral over L in Eq. (6.10) is negligible compared with the other two. In Eqs. (6.8) - (6.10) the term involving $k \frac{\partial (\ln \phi_a)}{\partial k_x}$ appears to dominate [except for $t \gg \tau_r$ in Eq. (6.8)]. This was pointed out by Milder¹⁸ in his discussion of spectral perturbations. For a spectrum of the form k^p the relative contribution of the first and last terms in Eq. (6.10) is approximately $\frac{1}{2p}$, which in two dimensions is .125.

For the parameters given by Eqs. (6.18) - (6.21), Eq. (6.15), for an adverse current becomes,

$$\begin{aligned} \left(\frac{\delta F}{F}\right)_{\text{resonant}} &= 1 - \exp\left[-K^2 \int d^2 L \phi_a(\vec{L}) \left\{1 - .01 \left(\frac{t}{\tau_r}\right) \sin k \xi\right\}\right] \\ &= 1 - \exp\left[-4k_z^2 \sigma_z^2 \cos^2 \theta_o \left\{1 - .01 \left(\frac{t}{\tau_r}\right) \sin k \xi\right\}\right] \quad (6.22) \end{aligned}$$

The nonresonant contribution to the variation in the clutter cross section is given by Eq. (6.10) with $k \gg k_r \sim L$

$$\left(\frac{\delta \phi}{\phi}\right)_{\text{nonresonant}} \approx -0.06 \cos kx \quad (6.23)$$

The $\frac{\partial}{\partial k_x} (\ln \phi_a)$ term provides the dominant contribution to the modulation. The fractional change in the clutter cross section using Eqs. (6.22) and (6.23) is

$$\frac{\delta \sigma}{\sigma} \approx 1 - .06 \cos kx - \exp\left[-4(k\sigma_z)^2 \cos^2 \theta_o \left\{1 - (.01) \left(\frac{t}{\tau_r}\right) \sin k \xi\right\}\right] \quad (6.24)$$

We see from Table I that $k\sigma_z$ for X-band radar is 1.88 for a Phillips spectrum, so that the resonant contribution is maximum for $\theta_0 \sim 0^\circ$ and/or early times. The fractional change in cross section for small angles of incidence is

$$\frac{\delta\sigma}{\sigma} \approx 1 - .06 \cos kx \quad (6.25)$$

so that the total cross section varies by a factor of two at X-band frequencies.

C-band radar, however, has $k\sigma_z = .0469$ for a Phillips spectrum so that for the same perturbing current

$$\frac{\delta\sigma}{\sigma} \approx -.06 \cos kx \quad (6.26)$$

and the variation in clutter cross section is 12% peak to peak.

Another source of variation in the clutter cross section is that due to changes in angle of incidence of the radar (ie., changes in surface slope). Labeling the fractional change in clutter cross section in Eq. (6.24) as being current induced, we write the total variation as

$$\frac{\delta\sigma}{\sigma} = \left(\frac{\delta\sigma}{\sigma} \right)_{\text{current induced}} + \left(\frac{\delta F}{F} \right)_{\text{rms slope}} \quad (6.27)$$

From Eqs. (4.15), (4.16) and Appendix B we have that the dependence of the long wave scattering on the angle of incidence is to lowest order in the rms slope

$$F(\vec{l}; \theta_0) \approx \left[\cos^4 \theta_0 + 2 \sin^2 \theta_0 \cos^2 \theta_0 \sigma_{z_x}^2 \right] \exp \left[-(1-E_z) (\kappa \sigma_z)^2 \right] \quad (6.28)$$

If we change our definition of incidence angle so as to be more appropriate for Bragg scattering $\theta_{inc} = \frac{\pi}{2} - \theta_{inc.}$, then

$$F(\vec{l}; \theta_{inc}) \approx \left[\theta_{inc}^4 + 2 \theta_{inc}^2 \langle z_x^2(\vec{\rho}) \rangle \right] \exp \left[-(1-E_z) (\kappa \sigma_z)^2 \right]. \quad (6.29)$$

The rms slope contribution to the perturbation in the clutter cross section is then given by

$$\begin{aligned} \left(\frac{\delta F}{F} \right)_{\text{rms slope}} &= \frac{2}{\theta_{inc}^2} \frac{\left[\langle z_x^2 \rangle_{\text{perturbed}} - \langle z_x^2 \rangle_{\text{unperturbed}} \right]}{\langle z_x^2 \rangle_{\text{unperturbed}}} \\ &= \frac{2}{\theta_{inc}^2} \frac{1}{N} \int k_x^2 \delta \phi(\vec{k}, \vec{x}) d^2 k \end{aligned} \quad (6.30)$$

where $\delta \phi(\vec{k}, \vec{x})$ is the current induced spectral perturbation and N is the integral over the unperturbed spectrum.

Again assuming a spectrum of the form (6.16) we have

$$\begin{aligned} N &= \frac{B}{\pi} \int_0^{2\pi} \int_{k_{\min}}^{k_{\max}} (k dk d\beta) \frac{k^2 \cos^2 \beta}{k^4} \\ &= B \ln \left(\frac{k_{\max}}{k_{\min}} \right). \end{aligned} \quad (6.31)$$

Assuming a modulation function $M(\vec{k}, \vec{x})$ such that

$$\delta\phi(\vec{k}, \vec{x}) = \phi_a(\vec{k}) M(\vec{k}, \vec{x}) \quad (6.32)$$

eq. (6.30) becomes

$$\left(\frac{\delta F}{F}\right)_{\text{rms slope}} = \frac{2}{\pi\theta_{\text{inc}}^2 \ln\left(\frac{k_{\text{max}}}{k_{\text{min}}}\right)} \int_{k_{\text{min}}}^{k_{\text{max}}} \int_0^{2\pi} M(\vec{k}, \vec{x}) \frac{dk}{k} \cos^2\beta \, d\beta \quad (6.33)$$

$$= -\frac{0.73 \times 10^{-3} \operatorname{sinc}\kappa\xi (t/\tau_r)}{\theta_{\text{inc}}^2 \ln\left(\frac{k_{\text{max}}}{k_{\text{min}}}\right)} \int_{k_{\text{min}}}^{k_{\text{max}}} \frac{dk}{k} \int_0^{2\pi} (\cos^2\beta - 8 \cos\beta) \cos^2\beta \, d\beta$$

$$\left(\frac{\delta F}{F}\right)_{\text{rms slope}} \approx -1.7 \times 10^{-3} \left(\frac{t}{\tau_r}\right) \frac{\operatorname{sinc}\xi}{\theta_{\text{inc}}^2} \quad (6.34)$$

or in terms of the current itself

$$\left(\frac{\delta F}{F}\right)_{\text{rms slope}} \approx -0.17 \left(\frac{t}{\tau_r}\right) \frac{U(\xi)}{\theta_{\text{inc}}^2} \quad (6.35)$$

The relative perturbation in the clutter cross section, therefore, falls off as θ_{inc}^2 and is proportional to the perturbing current.

VII. DISCUSSION AND CONCLUSIONS

The ocean surface has at least two classes of roughness: one class where $k\sigma_z > 1$ and one where $k\sigma_z < 1$. In the NELC Tower measurements, six radar frequencies (P, L, S, C, X, K) were used. For the sample scattering calculations, the nominal values $\lambda = 60$ cm (P), $\lambda = 6$ cm (C) and $\lambda = 1.5$ cm (X) were used. We assume that the ocean spectrum is a composite of the rough ocean (SWOP) and the slightly rough ocean encountered in the NELC measurements. If these types of roughness are present, they result in scattering having characteristics of each. To a good approximation, one can add the incoherent cross-sections directly to obtain the total incoherent cross-section if the processes are statistically independent. The large scale roughness produces strong components near normal incidence which are identical for vertical and horizontal polarization. This is the so-called quasi-specular component. Small scale roughness contributes to the tail (θ_0 near 90°) and is referred to as the diffuse component.

In Table I the statistical parameters for four ocean spectra and three radar wavelengths, including UHF, C band and X band are listed. From this Table it is clear that the applicability of a specific model, ie., set of assumptions for the radar scattering, is dependent on both the sea state and radar wavelength. In Table II the scattering models considered in this paper are listed where most appropriate for a particular sea state and radar wavelength.

TABLE II

RADAR WAVELENGTH	SCATTERING MODELS (SEA STATE)		
	SWOP	SRI	PHILLIP'S OR RRI
60 cm	Quasi-Specular $k\sigma_z \gg 1$, $k\ell \gg 1$ (rough sea)	Perturbation Theory $k\sigma_z \ll 1$, $\ell \ll 1$ (slightly rough sea)	Perturbation Theory $k\sigma_z \ll 1$, $\ell \ll 1$ (slightly rough sea)
6 cm	Quasi-Specular $k\sigma_z \gg 1$, $k\ell \gg 1$ (rough sea)	Physical Optics $k\sigma_z \ll 1$, $k\ell \gg 1$ (slightly rough sea)	Physical Optics $k\sigma_z \ll 1$, $k\ell \gg 1$ (slightly rough sea)
1.5 cm	Quasi-Specular $k\sigma_z \gg 1$, $k\ell \gg 1$ (rough sea)	Physical Optics $k\ell \gg 1$ (rough sea)	Physical Optics $k\sigma_z \ll 1$, $k\ell \gg 1$ (slightly rough sea)

The radar scattering models are listed for three radar wavelengths 60 cm, 6 cm, 1.5 cm and three surface wave spectra, which indicate the sea state. The models included in each box are selected by comparing the assumptions made with the statistical parameters presented in Table I.

From Section VI it is clear that the "visibility" of a surface wave spectral perturbation is dependent on the sea state and therefore on the radar frequency with which one views the sea surface. In the example considered the visibility of the current induced perturbation was reduced by an order of magnitude when one changed from X to C band radar in a Phillip's saturated sea.

The variation in the clutter cross section in lowest order consists of three terms,

$$\frac{\delta\sigma}{\sigma} = \left(\frac{\delta F}{F}\right)_{\text{resonant}} + \left(\frac{\delta\Phi}{\Phi}\right)_{\text{nonresonant}} + \left(\frac{\delta F}{F}\right)_{\text{rms. slope}}$$

The first term is the direct mechanical interaction of sea waves resonant with the surface current. The second term is the perturbation in the short surface waves due to both the nonresonant interaction with the current and wave-wave interactions of the scatterers with the sea waves. The final term is due to the variation in the angle between the sea waves and the incident radar and decreases as the inverse of the square of the angle of incidence.

REFERENCES

1. Callan, C. G. and R. Dashen, 1968: Inst. Def. Anal. Study S-334. Jason, Supporting Analysis D.
2. [REDACTED] *
3. Wright, J. W., 1968: IEEE Trans. Ant. and Prop. 16, 217
4. Cox, C. S. and W. H. Munk, 1954: J. Mar. Res. 14, 198.
5. Beckmann, P., 1965: IEEE Trans. Ant. and Prop. 13, 384
6. Bass, F. G., I. M. Fuks, A. I. Kalmykov, I. E. Ostrovsky and A. D. Rosenberg, 1968: IEEE Trans. Ant. and Prop. 16, 554.
7. Watson, K.M. and B. J. West, 1974: Physical Dynamics Report, PD-74-064, RADC-TR-74-267
8. Jarem, J., 1964: Re-entry Analysis Test Measurements 68-08, ARPA Order (51), DA-01-021-AMC-12963(3)
9. Neumann, G. and W. J. Pierson Jr., 1966: Principles of Physical Oceanography, Prentice-Hall Inc., 350
10. Hasselmann, K., 1968: Basic Developments in Fluid Mechanics, (ed. M. Holt), 2, 117 (Academic Press)
11. Watson, K. M., and B. J. West, 1975: J. Fluid Mech., 70, 815
12. Thomson, J.A.L. and B. J. West, 1973: Physical Dynamics Report PD-72-029, RADC-TR-73-192
13. Phillip's, O. M., 1966: The Dynamics of the Upper Ocean, Cambridge University Press, Sec. 4.5
14. Op. Cit. ref. (9), pps. 352-357
15. [REDACTED] *
16. Thomson, J.A.L. and B. J. West, 1972: Physical Dynamics Report, PD-72-023, RADC-TR-72-280
17. Case, K. M., K. M. Watson and B. J. West, 1973: Physical Dynamics Report, PD-73-047, RADC-TR-74-110.
18. Watson, K.M. and B. J. West, 1974: Physical Dynamics Report PD-73-050, RADC-TR-74-42
19. M. Milder, private communication

*Supplied to qualified requesters.

Appendix A - Effect of Diffraction

To estimate the effect of diffraction on shadowing, consider a plane wave incident on a sinusoidal surface of amplitude H . For a horizontally propagating scalar wave with incident amplitude ψ_0 , the scattered wave is

$$\psi = \psi_0 e^{-i\pi/4} \int_{z_s}^{\infty} \exp\left[i\pi(y-y')^2/\lambda_r \Delta x\right] \frac{dy}{\sqrt{\lambda_r \Delta x}} \quad (A1)$$

which is the Fresnel expression for scattering from a knife edge. The position of the surface is z_s and Δx is the distance the wave has propagated. The wave spreads due to diffraction like

$$i\pi(z-z_s)^2/\lambda_r \Delta x \sim i\pi \quad (A2)$$

so that

$$z - z_s = \pm \sqrt{\lambda_r \Delta x} \quad (A3)$$

This defines a parabola within the geometric shadow which is illuminated due to diffraction.

The maximum area illuminated due to diffraction would be twice the wave height, located at the wave trough, i.e., $\Delta x = \lambda_{\text{sea}}/2$, therefore,

$$2H = \sqrt{\lambda_r \Delta x} = \sqrt{\lambda_r \lambda_{sea}} / 2 \quad . \quad (A4)$$

This equation establishes criteria for the threshold of shadowing, that is,

$$\begin{aligned} 8H^2/\lambda_r > \lambda_{sea} &: \text{illuminated} \\ & \text{(no shadow)} \\ 8H^2/\lambda_r \gg \lambda_{sea} &: \text{geometric optics} \\ & \text{(no diffraction)} \quad . \quad (A5) \end{aligned}$$

In terms of oceanographic parameters, such as the slope $\theta_{sea} = 2\pi H/\lambda_{sea}$, we can write

$$\lambda_r/\lambda_{sea} < \frac{8}{4\pi^2} \textcircled{\#}_{sea}^2 \approx \frac{1}{5} \textcircled{\#}_{sea}^2 \quad (A6)$$

where the rms slope $\textcircled{\#}_{sea}$ has replaced that for a single wave θ_{sea} . For a saturated sea

$$\textcircled{\#}_{sea}^2 = .006 \log \left(\frac{k_{max}}{k_{min}} \right) \quad (A7)$$

so that reasonable numbers for the mean square slope are like .025 to .05. Substituting these values into Eq. (A6) yields $.005 \leq \lambda_r/\lambda_{sea} \leq .01$, so that for X-band radar ($\lambda_r \sim 3$ cm) the sea waves which give shadowing are ≥ 3 to meters. These criteria establish the region of the wave-number spectrum, below which shadowing can be neglected due to diffraction.

Appendix B - Averages of Statistically-Separable Surfaces

Consider the average of the series expansion of the characteristic function,

$$\begin{aligned} \langle \exp [iK(Z-Z')] \rangle &= 1 + iK \langle Z-Z' \rangle - \frac{K^2}{2} \langle (Z-Z')^2 \rangle \\ &\quad - i \frac{K^3}{6} \langle (Z-Z')^3 \rangle + \frac{K^4}{24} \langle (Z-Z')^4 \rangle + \dots \end{aligned} \quad (B1)$$

The odd moments in B1 vanish for a Gaussian distribution and

$$\begin{aligned} \langle (Z-Z')^2 \rangle &= 2\sigma_z^2 [1 - E_z(\vec{\rho}-\vec{\rho}')] \\ \langle (Z-Z')^4 \rangle &= 12\sigma_z^4 [1 - E_z(\vec{\rho}-\vec{\rho}')]^2 \end{aligned}$$

so that the series expansion becomes

$$\langle \exp[iK(Z-Z')] \rangle = 1 - (K\sigma_z)^2 (1 - E_z) + \frac{(K\sigma_z)^4}{2} (1 - E_z)^2 + \dots \quad (B2)$$

It is clear that the series in B2 can be summed to yield the exact result

$$\langle \exp [iK(Z-Z')] \rangle = \exp \left[-(K\sigma_z)^2 (1 - E_z) \right] . \quad (B3)$$

Similar exact calculations may be made to obtain the following results;

$$\langle (z_x + z'_{x'}) \exp[iK(z-z')] \rangle = -i2K\sigma_z^2 \frac{\partial E_z}{\partial x} \exp[-(K\sigma_z)^2(1-E_z)] \quad (\text{B4})$$

$$\langle (z_x^2 + z'_{x'}{}^2) \exp[iK(z-z')] \rangle = 2 \left[\sigma_z^2 - (K\sigma_z)^2 \sigma_z^2 \left(\frac{\partial E_z}{\partial x} \right)^2 \right] \exp[-(K\sigma_z)^2(1-E_z)] \quad (\text{B5})$$

$$\begin{aligned} \langle z_x z'_{x'} (z_x + z'_{x'}) \exp[iK(z-z')] \rangle \\ = i2K\sigma_z^2 \frac{\partial E_z}{\partial x} \left[-\sigma_z^2 + (K\sigma_z)^2 \sigma_z^2 \left(\frac{\partial E_z}{\partial x} \right)^2 + 2\sigma_z^2 \frac{\partial^2 E_z}{\partial x^2} \right] \exp[-(K\sigma_z)^2(1-E_z)] \end{aligned} \quad (\text{B6})$$

$$\begin{aligned} \langle z_x^2 z'_{x'}{}^2 \exp[iK(z-z')] \rangle = & \left[\sigma_z^4 + 2\sigma_z^4 \left(\frac{\partial^2 E_z}{\partial x^2} \right)^2 + 4(K\sigma_z)^4 \sigma_z^4 \frac{\partial^2 E_z}{\partial x^2} \left(\frac{\partial E_z}{\partial x} \right)^2 \right. \\ & \left. + (K\sigma_z)^4 \sigma_z^4 \left(\frac{\partial E_z}{\partial x} \right)^4 - 2(K\sigma_z)^2 \sigma_z^2 \sigma_z^2 \left(\frac{\partial E_z}{\partial x} \right)^2 \right] \\ & \times \exp[-(K\sigma_z)^2(1-E_z)] \end{aligned} \quad (\text{B7})$$

$$\langle z_x z'_{x'} \exp[iK(z-z')] \rangle = - \left[\sigma_z^2 \frac{\partial^2 E_z}{\partial x^2} + (K\sigma_z)^2 \sigma_z^2 \left(\frac{\partial E_z}{\partial x} \right)^2 \right] \exp[-(K\sigma_z)^2(1-E_z)] \quad (\text{B8})$$

C. PHYSICAL OPTICS SCATTERING FOR A ROUGH SEA

In Ref. (8) the physical optics approximation was used to evaluate the Stratton-Chu scattering integral. This tangent-plane approximation requires the radius of curvature at all points of the sea surface to be greater than the radar wavelength λ_r . No restriction was made concerning the mean square roughness height compared to λ_r , in contrast to Ref. (1) where $H/\lambda_r \ll 1$. Otherwise the model is similar to that described in the previous sections, i.e., any correlation lengths are much greater than the wavelengths of the scattering centers. For a Gaussian correlation function, it is possible to evaluate the incoherent scattering cross section exactly. The resultant backscatter cross section per unit area is, using ℓ as a correlation length,

$$\frac{\sigma_I}{S} = (k\ell)^2 \sec^2 \theta_0 \psi(\alpha, \beta)$$

$$\alpha = (2k\sigma_z \cos \theta_0)^2$$

$$\beta = (k\ell \sin \theta_0)^2$$

$$\psi(\alpha, \beta) = \exp(-\alpha) \sum_{n=1}^{\infty} \frac{\alpha^n}{n!n} \exp(-\beta/n). \quad (C1)$$

Figure 8 depicts the incoherent scattering function $\psi(\alpha, \beta)$ extracted from Ref. (8).

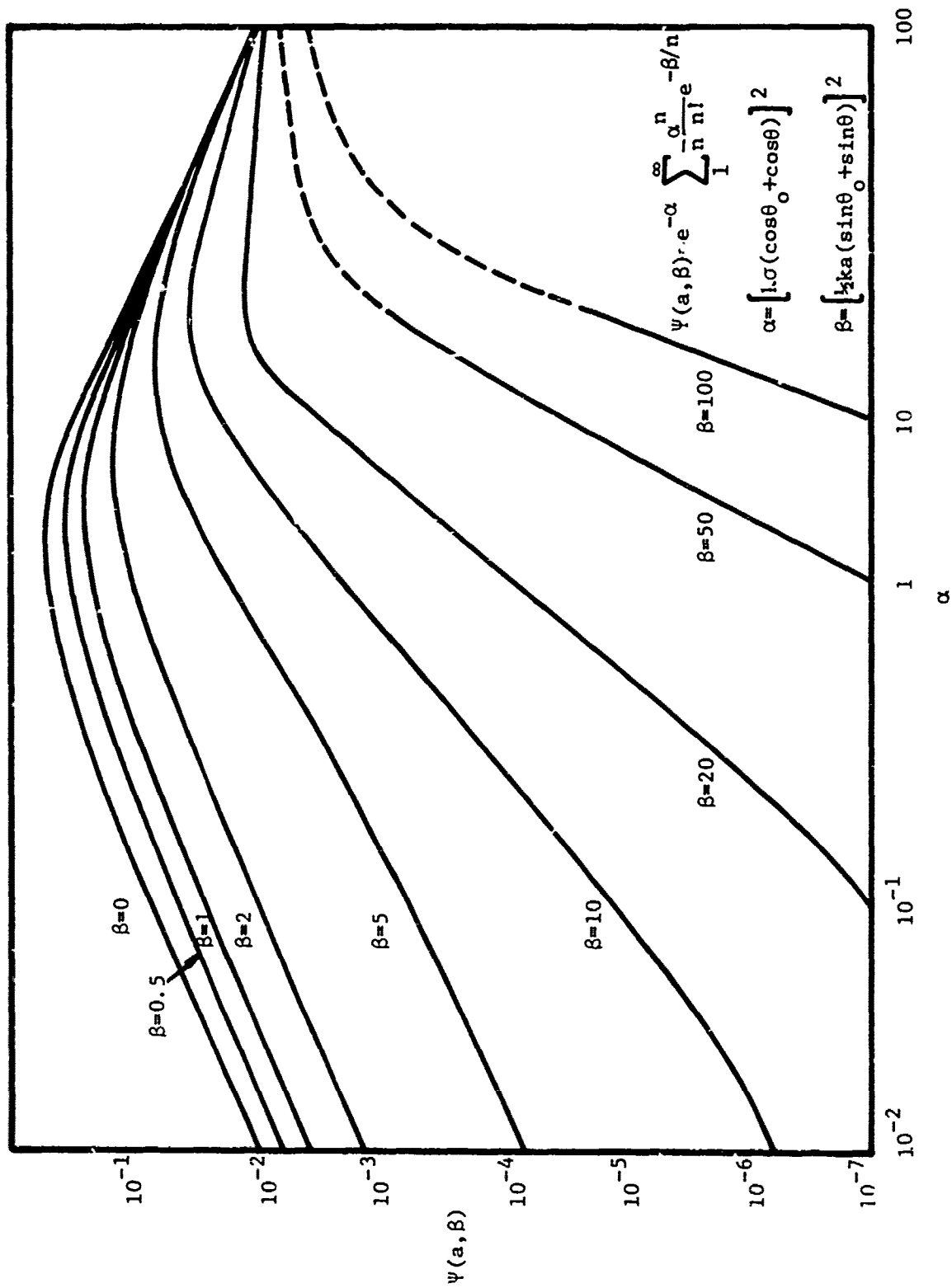


FIG. 8 INCOHERENT SCATTERING FUNCTION FOR A SURFACE WITH A GAUSSIAN CORRELATION FUNCTION

D. PERTURBATION THEORY FOR SCATTERING FROM A SLIGHTLY ROUGH OCEAN

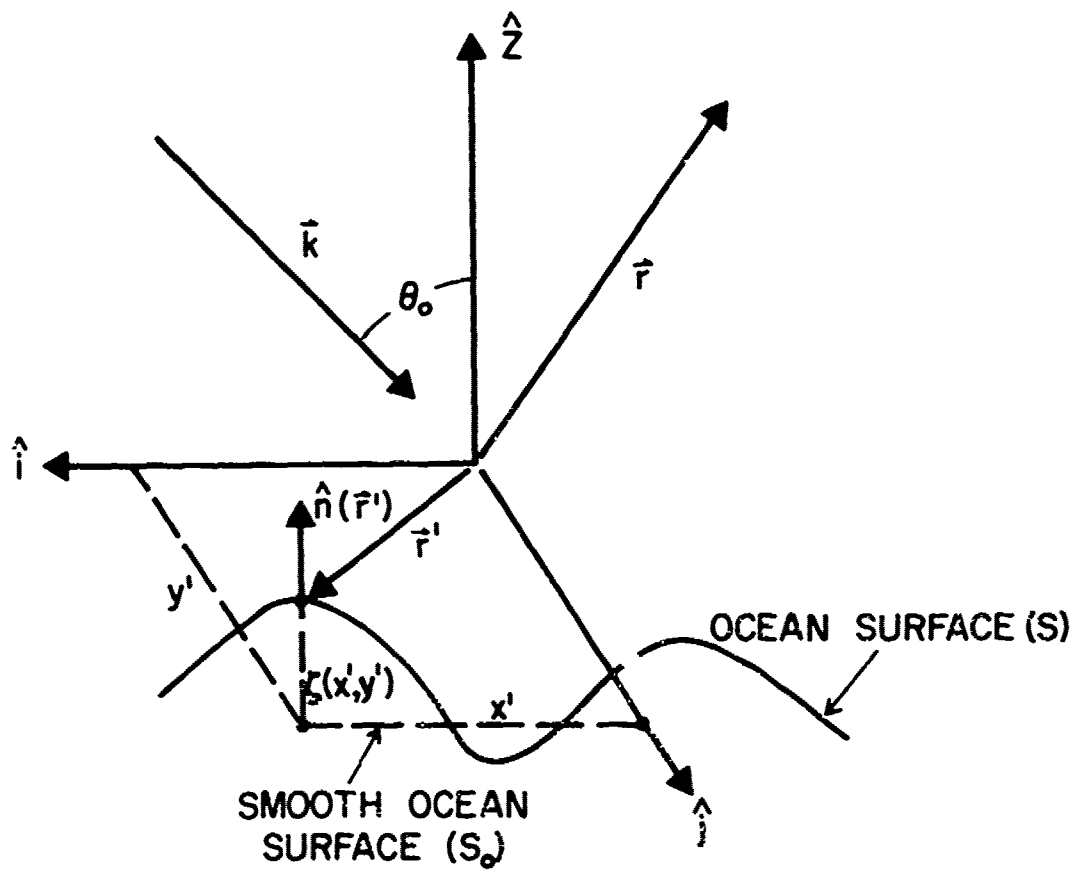
In previous sections, the physical optics approximation was made which is valid when the radius of curvature of the ocean surface is large compared to the radar wavelength. In this section we relax this assumption and require that the roughness height be small ($k\sigma_z \ll 1$) and that the surface slopes be relatively small ($\nabla\zeta < 1$). A smoothly-curving surface with small slope will satisfy the physical optics radius of curvature requirement for the high-frequency limit but eventually this condition will fail as the frequency is decreased.

Consider the scattering geometry shown in Figure 9. For small surface fluctuations (S) about the reference ocean surface (S_0), we expect small perturbations in the scattered field. When S_0 is illuminated by a plane wave

$$\vec{E}_j(\vec{r}) = (\hat{x}A_1 + \hat{y}A_2 + \hat{z}A_3) \exp(-i\vec{k}\cdot\vec{r}) \quad , \quad \vec{k} = (k_1, k_2, k_3) \quad (D1)$$

then the scattered field is (with S_0 large and infinite ocean conductivity)

$$\vec{E}_s(\vec{r}) = (-\hat{x}A_1 - \hat{y}A_2 + \hat{z}A_3) \exp[-i(k_1x + k_2y - k_3z)] \quad . \quad (D2)$$



SCATTERING GEOMETRY WITH INCIDENT WAVE IN THE
 (X,Z) PLANE AND A SMOOTH OCEAN SURFACE (S_0)
 AND DISPLACED SURFACE (S)

FIG. 9

This solution satisfies the tangential boundary conditions

$$\hat{z} \times \vec{E} = 0 \quad \text{on } S_0, \quad \vec{E} = \vec{E}_0 + \vec{E}_s$$

or

$$-\hat{z} \times \vec{E}_s(\vec{r}'_0) = \hat{z} \times \vec{E}_0(\vec{r}'_0) - \vec{K}_m^{(0)}; \quad \vec{r}'_0 \in S_0 \quad (\text{D3})$$

We can also view the above scattering problem in the following way. The incident field \vec{E}_0 induces a magnetic current $\vec{K}_m^{(0)}$ on the surface S_0 which gives rise to a field above the surface. The total scattered field is obtained by summing all such magnetic surface currents over S_0 . This is facilitated by using the magnetic dyadic Green's function for a half plane

$$\vec{E}_s(\vec{r}) = -2\nabla \times \int_{S_0} dS \left(\vec{I} + \frac{\nabla \nabla}{k^2} \right) \frac{\exp[-ik|r-r'|_0]}{4\pi|\vec{r}-\vec{r}'_0|} \cdot (\hat{x}\hat{x} + \hat{y}\hat{y}) \cdot \vec{K}_m^{(0)}(\vec{r}'_0) \quad (\text{D4})$$

When the surface is rough the scattered field will be perturbed from that given by Eq. (D4). We calculate the perturbed field by finding the equivalent surface currents on S_0 which account for the current on S at the height

$$z = \zeta(x', y') = \zeta(r'_0) \quad .$$

The currents on S_0 are found by using a perturbation expansion of the scattered field in powers of the surface

height ζ . This expansion satisfies the boundary condition

$$\hat{n}(\vec{r}') \times [\vec{E}_s(\vec{r}') + \vec{E}_i(\vec{r}')] = 0$$

Let the scattered field be represented by the series

$$\vec{E}_s(\vec{r}') = \sum_{n=0}^{\infty} \vec{E}^{(n)}(\vec{r}') \quad ; \quad |\vec{E}^{(n)}| \sim |\zeta|^n \quad (D5)$$

where each $\vec{E}^{(n)}$ satisfies Maxwell's equations. In addition, each term will be expanded in a Taylor series about \vec{r}'_0 .

To first order the scattered field is

$$\vec{E}_s(\vec{r}') \approx \vec{E}^{(0)}(\vec{r}'_0) + \zeta \frac{\partial}{\partial z'} \vec{E}^{(0)}(\vec{r}'_0) + \vec{E}^{(1)}(\vec{r}'_0)$$

$$\vec{E}^{(0)}(\vec{r}') = \vec{A} \exp(i\vec{k} \cdot \vec{r}') \approx \vec{A}(1 - ik_z \zeta) \exp(-i\vec{k} \cdot \vec{r}'_0). \quad (D6)$$

With the equation for the free surface $z' - \zeta(x', y') = 0$, the unit vector normal to this surface is to first order

$$\hat{n}(\vec{r}') = \frac{\nabla'(z' - \zeta)}{|\nabla'(z' - \zeta)|} = \frac{\hat{z} - \hat{x}\zeta_x - \hat{y}\zeta_y}{|\hat{z} - \hat{x}\zeta_x - \hat{y}\zeta_y|} \approx \hat{z} - \hat{x} \frac{\partial \zeta}{\partial x'} - \hat{y} \frac{\partial \zeta}{\partial y'}. \quad (D7)$$

When Eqs. (D6) and (D7) are used in the tangential boundary conditions

$$\hat{n} \times [\vec{A} \exp(-i\vec{k} \cdot \vec{r}'_0) + \vec{E}^{(0)}(\vec{r}'_0)] = 0$$

we obtain

$$\begin{aligned} \hat{z} \times \left[-ik_3 \zeta \vec{A} \exp(-i\vec{k} \cdot \vec{r}'_0) + \zeta \frac{\partial}{\partial z'} \vec{E}^{(0)}(\vec{r}'_0) + \vec{E}^{(1)}(\vec{r}'_0) \right] \\ = (\hat{i}\zeta_x + \hat{j}\zeta_y) \times \left[\vec{A} \exp(-i\vec{k} \cdot \vec{r}'_0) + \vec{E}^{(0)}(\vec{r}'_0) \right] \quad (D8) \end{aligned}$$

From Eq. (D8) we readily calculate

$$\hat{z} \times \vec{E}^{(1)}(\vec{r}'_0) = 2 \left[ik_3 \zeta (\hat{y}A_1 - \hat{x}A_2) + A_3 (\hat{x}\zeta_y - \hat{y}\zeta_x) \right] \exp(-i\vec{k} \cdot \vec{r}'_0) \quad (D9)$$

The first order magnetic current is then

$$\vec{K}_m^{(1)}(\vec{r}'_0) = 2 \left[\hat{x}(-ik_3 \zeta A_2 + A_3 \zeta_y) + \hat{y}(ik_3 \zeta A_1 + A_3 \zeta_x) \right] \exp(-i\vec{k} \cdot \vec{r}'_0) \quad (D10)$$

which could be used in Eq. (D4) to calculate $\vec{E}^{(1)}(\vec{r})$.

However, it will be more convenient to calculate the magnetic field using

$$\vec{H}_s(\vec{r}) = \frac{2k^2}{i\omega\mu} \int_{S_0} dS \left(\hat{T} + \frac{\nabla\nabla}{k^2} \right) G(\vec{r}-\vec{r}'_0) \cdot (\hat{x}\hat{x} + \hat{y}\hat{y}) \cdot \vec{K}_m(\vec{r}'_0) \quad (D11)$$

Using the far field approximation to simplify the Green's function in Eq. (D11) along with Eq. (D10), we obtain for a rectangular surface ($S_0 = x_0 y_0$)

$$\vec{H}^{(0)}(\vec{r}) = \frac{k^2 x_0 y_0}{2\pi i \omega \mu} \frac{\exp(-ikr)}{r} \text{sinc}\left(q_1 \frac{x_0}{2}\right) \left(\hat{T} - \hat{r}\hat{r} \right) \cdot (\hat{i}A_2 - \hat{j}A_1) \quad (D12)$$

where

$$\vec{q} = \hat{x}q_1 + \hat{y}q_2, \quad q_1 = k_1 - k\hat{r} \cdot \hat{x}, \quad q_2 = k_2 - k\hat{r} \cdot \hat{y}. \quad (D13)$$

Using the spectral representation for the random surface displacement

$$\zeta(\vec{r}'_0) = \int_{-\infty}^{\infty} d\phi(\vec{k}) \exp(-i\vec{k} \cdot \vec{r}'_0), \quad \vec{k} = \hat{x}\kappa_1 + \hat{y}\kappa_2$$

and the vector $\vec{B}(\vec{k})$ defined by

$$\vec{B}(\vec{k}) = \hat{x}B_1 + \hat{y}B_2 = \hat{x}(k_3A_2 + A_3\kappa_2) - \hat{y}(k_3A_1 + A_3\kappa_1) \quad (D14)$$

the next order term in the expansion of the magnetic field is

$$\begin{aligned} \vec{H}^{(1)}(\vec{r}) &= \frac{-2k^2}{2\pi\omega\mu} \frac{\exp(-ikr)}{r} (\vec{I} - \hat{r}\hat{r}) \cdot \int_{S_0} dS \exp(ik\hat{r} \cdot \vec{r}') \int_{-\infty}^{\infty} d\phi(\vec{k}) \vec{B}(\vec{k}) \\ &\times \exp(-i(\vec{k} + \vec{k}) \cdot \vec{r}'_0) \end{aligned} \quad (D15)$$

carrying out the surface integration in (D15), we find for the integral terms, call it the vector $\vec{D}(\hat{r})$,

$$\vec{D}(\hat{r}) = x_0 y_0 \int_{-\infty}^{\infty} d\phi(\vec{k}) \vec{B}(\vec{k}) \text{sinc}\left[(q_1 - \kappa_1) \frac{x_0}{2}\right] \text{sinc}\left[(q_2 - \kappa_2) \frac{y_0}{2}\right] \quad (D16)$$

and

$$\vec{H}^{(1)}(\vec{r}) = \frac{-2k^2}{2\pi\omega\mu} \frac{\exp(-ikr)}{r} (\vec{I} - \hat{r}\hat{r}) \cdot \vec{D}(\hat{r}) \quad (D17)$$

The radar cross section in terms of the magnetic field is, to first order,

$$\sigma = 4\pi r^2 \frac{\langle \vec{H}_s \cdot \vec{H}_s^* \rangle}{|H_0|^2} \approx \frac{4\pi r^2}{H_0^2} \left[|\vec{H}^{(0)}|^2 + \langle |\vec{H}^{(1)}|^2 \rangle \right] \quad (D17)$$

where $\langle \vec{H}^{(1)} \rangle = 0$ and $H_0^2 = \frac{\epsilon}{\mu} E^2$.

The first order contribution to the cross section is

$$\sigma^{(1)} = \frac{4k^2}{\pi E_0^2} \left(\langle |\vec{D}|^2 \rangle - \langle |\vec{E} \cdot \vec{D}|^2 \rangle \right) \quad (D19)$$

where

$$\begin{aligned} \langle |\vec{D}|^2 \rangle &= (x_0 y_0)^2 \int_{-\infty}^{\infty} \langle d\phi(\vec{k}) d\phi^*(\vec{k}') \rangle \vec{B}(\vec{k}) \cdot \vec{B}(\vec{k}') \\ &\times \text{sinc} \left[(q_1 - \kappa_1) \frac{x_0}{2} \right] \text{sinc} \left[(q_2 - \kappa_2') \frac{y_0}{2} \right]. \quad (D20) \end{aligned}$$

For a spatially-homogeneous spectrum of ocean surface waves

$$\langle d\phi(\vec{k}) d\phi^*(\vec{k}') \rangle = d\vec{k} d\vec{k}' \phi(\vec{k}) \delta(\vec{k} - \vec{k}') \quad (D21)$$

When Eq. (D21) is used in Eq. (D20) and the ocean spectrum does not change too rapidly about \vec{q} , then the approximate value of integral (D20) is

$$\langle |\vec{D}|^2 \rangle \approx |\vec{E}(\vec{q})|^2 \phi(\vec{q}) (2\pi)^2 x_0 y_0 . \quad (D22)$$

Similarly,

$$\langle |\hat{r} \cdot \vec{D}|^2 \rangle \approx |\hat{r} \cdot \vec{E}(\vec{q})|^2 \phi(\vec{q}) (2\pi)^2 x_0 y_0 . \quad (D23)$$

$\sigma^{(1)}$ then becomes

$$\sigma^{(1)} = \frac{4k^2}{\pi E_0^2} (2\pi)^2 x_0 y_0 \left[|\vec{E}(\vec{q})|^2 - |\hat{r} \cdot \vec{E}(\vec{q})|^2 \right] \phi(\vec{q}) . \quad (D24)$$

We now specialize to backscatter ($\hat{r} = -\hat{k}$) and horizontal polarization with

$$\vec{E}_0 = \hat{j} A_2$$

$$A_1 = A_3 = 0$$

$$k_1 = -k \sin\theta_0, \quad k_2 = 0, \quad k_3 = -k \cos\theta_0 .$$

From Eq. (D13)

$$q_1 = k_1 - k\hat{r} \cdot \hat{x} = -2k \sin\theta_0$$

$$q_2 = k_2 - k\hat{r} \cdot \hat{y} = 0$$

and Eq. (D14)

$$B_1(\vec{q}) = k_3 A_2 + A_2 q_2 = -k \cos \theta_0 E_0$$

$$B_2(\vec{q}) = k_3 A_1 + A_3 q_1 = 0 \quad .$$

Substituting the above conditions for backscattering in Eq. (56) yields the first order incoherent cross section per unit area for horizontal polarization

$$\frac{\sigma^{(1)}}{x_0 y_0} = 16 \pi k^4 \cos^4 \theta_0 \phi(-2k \sin \theta_0, 0) \quad . \quad (D25)$$

Next we specialize to backscatter and vertical polarization for which $\vec{E}_0 = \hat{x}A_1 + \hat{z}A_3$ and $A_2 = 0$, all other quantities being the same as in the preceding example. With these values the incoherent cross section per unit area for vertical polarization is

$$\frac{\sigma^{(1)}}{x_0 y_0} = 16 \pi k^4 (1 + \sin^2 \theta_0)^2 \phi(-2k \sin \theta_0, 0) \quad . \quad (D26)$$

Using Eq. (D12) for $\vec{H}^{(0)}$, we determine the zeroth order, or coherent cross section for both vertical and horizontal polarization, to be

$$\frac{\sigma^{(0)}}{x_0 y_0} = (k x_0 y_0)^2 \cos^2 \theta_0 \text{sinc}(k x_0 \sin \theta_0) \quad . \quad (D27)$$

E. QUASI-SPECULAR SCATTERING FROM VERY ROUGH SEA

When surface roughness is large compared to radar wavelength ($k\sigma_z \gg 1$), the scattered power becomes more incoherent. For $k_r \zeta > 5$, k_r being the radar wavenumber $2\pi/\lambda_r$, the coherent power is negligible. The following analysis assumes that all scattering comes from specular reflections so that the backscattered power is perfectly reflected and consequently there is no cross polarization.

When surface roughness is isotropic, the correlation length for surface waves is much less than either dimension of the illuminated area. Neglecting multiple scattering and shadowing allows for stationary-phase integration of the surface scattering integral. This integration yields the incoherent backscattering cross section per unit area:

$$\frac{\sigma_I}{S} = \frac{\sec^4 \theta_0}{\textcircled{1}^2_{\text{sea}}} \exp(-\tan^2 \theta_0 / \textcircled{2}_{\text{sea}}) \quad (E1)$$

where

$$\textcircled{1}^2_{\text{sea}} \equiv \left(\frac{2\sigma_z}{\ell} \right)^2 \text{ is the mean square total slope of the rough surface}$$

$$\ell \equiv \text{correlation length for } \rho(r) = e^{-r^2/\ell^2} \approx 1 - \frac{r^2}{\ell^2}$$

$$r \equiv \left[(x_1 - x_2)^2 + (y_1 - y_2)^2 \right]^{1/2}$$

for a Gaussian surface-height joint probability density.